

SEARCHING FOR BROWN DWARF BINARIES USING GAIA, UKIRT AND SPEX

Jarrold Hansen

Department of Physics & Astronomy, N283 ESC, Brigham Young University, Provo, UT 84602, USA

A senior thesis submitted to the faculty of
Brigham Young University
in partial fulfillment of the requirements for the degree of
Bachelor of Science

Denise Stephens, Advisor

Department of Physics and Astronomy
Brigham Young University
April 2021

Copyright © 2021 Jarrod Hansen

All Rights Reserved

Abstract

Searching for Brown Dwarf Binaries using GAIA, UKIRT and SpeX

Jarrod Hansen

Department of Physics and Astronomy

Brigham Young University

Historically Brown Dwarf Binaries have been discovered utilizing large amounts of time on ground or space-based telescopes to determine the orbits of closely spaced objects. This makes these discoveries hard to accomplish as you have to spend several nights of observing on a single object in the hope that it is a binary system. We examine utilizing distance measurements from GAIA and UKIRT to trim down target lists and identify the best binary candidates. We examine a sample of known binaries to determine how effective our method is at identifying known systems. We determine that luminosity measurements using distances are a good indicator for binarity.

Keywords: brown dwarfs, Binary Systems, Overluminosity

Acknowledgments

We would like to acknowledge the help of BYU faculty and students who have made this project possible. In particular we would like to thank Justin Tackett, Dr. Eric Hintz, John Michael Eberhard and my advisor Dr. Denise Stephens.

Contents

List of Figures	vi
1. Introduction	1
1.1. Brown Dwarfs	1
1.1.1. Formation Ideas and The Initial Mass Function	2
1.1.2. Spectral Types	5
1.1.3. Brown Dwarf Archives	7
1.2. Historical Binary Searches	7
1.2.1. Observing Brown Dwarfs with The Hubble Space Telescope	8
1.2.2. Ground-based Searches for Binary Brown Dwarfs	8
1.3. Telescope Systems and Archival Data	9
1.3.1. Global Astrometric Interferometer for Astrophysics (GAIA)	9
1.3.2. United Kingdom Infra-Red Telescope (UKIRT)	9
1.3.3. Infrared Telescope Facility (IRTF) SpeX Spectrometer	11
1.3.4. NASA Infrared Science Archive (IRSA)	12
1.3.5. The Two Micron All Sky Survey and Wide-Field Infrared Survey Explorer (2MASS and WISE)	12
2. Methods and Procedures	13
2.1. Using GAIA for brown dwarfs	13
2.1.1. Using Optical Imagers for IR objects	14
2.1.2. Object Searching using IRSA	16
2.1.3. Verifying GAIA data	20

2.1.4. Absolute Magnitudes from GAIA	22
2.2. Hawaii Infrared Parallax Program	23
2.3. Infrared Magnitudes from 2MASS and WISE	25
2.3.1. Source Verification	29
3. Identifying Overluminous Candidate Binaries	30
3.1. Binaries candidates	34
3.2. Identifying Known Binaries	37
3.2.1. Unresolved Binary Systems	38
3.3. Finding Spectral Binaries using Theoretical models	39
3.3.1. Agreement with Overluminosity	40
3.4. New Brown Dwarf Archive	41
3.4.1. New Data from GAIA, UKIRT, 2MASS and WISE	41
3.4.2. Availability and Utility	41
3.5. Absolute Magnitude as a Binary Indicator	42
3.5.1. Effectiveness of GAIA and UKIRT Parallax Measurements	42
3.5.2. Issues in Utilization of Archival Data	42
3.5.3. Future Possibilities with GAIA DR3	43
3.6. Conclusions	43

List of Figures

1	Initial Mass Function	5
2	Parallax Using Earths Orbit	10
3	Comparison between GAIA and UKIRT data.....	11
4	GAIA Passbands	16
5	Infrared Brown Dwarf image	17
6	Optical Brown Dwarf image.....	18
7	GAIA Searching.....	18
8	IRSA Searching	20
9	Search Results	21
10	Data Validation 1, g apparent magnitude vs Parallax error	22
11	Data Validation 2, Optical spectral type vs Parallax error	23
12	Data Validation 3, g Absolute magnitude vs Infrared spectral type	24
13	2MASS Filter profiles	27
14	WISE Filter profiles	28
15	Results 1, J magnitude variation within optical spectral types	31
16	Results 2, J magnitude variation within infrared spectral types	33
17	Results 3, Overluminosity in specific filters	33
18	Results 4, Overluminosity using WISE.....	34
19	Jupiter in Infrared from Gemini	36
20	Spectra nSB thresholds.....	40

1. INTRODUCTION

1.1. Brown Dwarfs

Brown dwarfs comprise an astronomical classification of objects that is generally defined in two ways. The first is a mass limiting range whose lower limit comes from the required mass to burn deuterium in the cores of these objects (Burrows et al. 2001). The upper limit of this mass range is the mass required to begin hydrogen fusion in the core. This constrains brown dwarfs to an upper mass limit of 0.078 Solar Masses, where a solar mass is the current mass of the sun, and a lower limit of 0.013 Solar Masses (Burrows et al. 2001). The second definition relates to the formation of the object and classifies brown dwarfs as objects that formed through a gravitational instability as opposed to core accretion in a disk around a star. This definition requires brown dwarfs form through gravitational collapse, the same formation mechanism as stars. This definition distinguishes them from planets that form through accretion of material in disks surrounding stars. Determining the formation path an individual brown dwarf evolved along is not possible so we will use the mass limiting range as our definition of a brown dwarf throughout this thesis.

Without fusion to support its structure brown dwarfs begin to collapse due to their gravitational pull after formation. This collapse continues until the density of materiel is high enough for the electron degeneracy pressure to support the structure. After this initial period of collapse the brown dwarf will continue to shrink and cool. This means that the luminosity of a brown dwarf will depend on its initial mass and age as the initial mass determines when electron degeneracy kicks in and their age determines how long they have been cooling for. The hottest brown dwarfs reach temperatures slightly above 3000 K while the coldest brown dwarf recorded has a temperature of 250 K (Kirkpatrick et al. 2021). These cool temperatures allow for chemical reactions with stable products in the upper atmospheres of the Brown Dwarf that produce identifiable spectral features.

The molecules that are produced depend on the temperature and pressure of the atmosphere of the brown dwarf so these features are used to classify different types of brown dwarfs.

1.1.1. Formation Ideas and The Initial Mass Function

Star formation occurs when large clouds of dust and gas collapse. From the collapse of a single cloud many stars are formed as the cloud fragments into smaller pieces each of which can result in the formation of single or multi-star systems. Observations of star forming regions have revealed that many more low mass stars are formed than high mass objects. The Initial Mass function (IMF) is used to describe the number of stellar objects as a function of mass. Several models of the initial mass function are shown in figure 1.

Uncertainties in the IMF are prominent at the low and high mass ends. This occurs because high mass stars have lifetimes that are comparable to the formation times of low mass stars. This leads to uncertainties of the numbers high mass objects as many of the high mass stars will have died before the cluster is examined. Looking at even younger clusters allows for better counts of high mass stars but the uncertainties in the low mass end go up as not all of the objects in that region would have formed. Figure 1 shows how the number of stars increases as mass decreases. At around the cutoff for the transition to brown dwarfs the stellar mass function drops off and there are much fewer objects than we would expect if the stellar mass function continued. Many attempts have been made to model this downturn but the low mass end of the IMF these models tend to disagree in the low mass regime (Chabrier 2003). This occurs, in part, because of the inability to get accurate counts of low mass objects because of their low luminosity that makes them impossible to detect in some of these surveys.

To understand the low mass end of the IMF we need an accurate count of all stars and low mass objects in a cluster. This would allow differentiation between the models in this low mass regime to determine which of our models is correct. Using these models we could then estimate what fraction of brown dwarfs we are not bright enough to be visible to our telescopes. Each model also has different assumptions about fragmentation, gas collapse and ejection rate that would effect our understanding of how brown dwarfs would form (Kirkpatrick et al. 2019). Improving the depth of our observations will allow us to improve how well our models match the data which will improve our understanding of the formation rates of low mass objects. Matching the models to improved data will also allow us to understand the binary fraction of these objects.

The computational models that are used to estimate the initial mass function also produce a binary mass fraction that describes what fraction of objects at given mass will form in binary systems. This fraction is the number of objects of a given mass that are found in binary systems, as well as the relative mass ratio of the primary and secondary component in those systems. Observations of multi-body systems have found that brown dwarfs are not found frequently found in binary systems with main sequence stars. Instead they are found almost exclusively in systems with another brown dwarf. This is in sharp contrast with observed fractions for low mass stars which are frequently found with a massive companion. The number of systems of binary brown dwarfs that form and the mass fractions of these systems place strong constraints on the computational models that try to reproduce the observed values for the initial mass function and the binary fraction (Bates 2000).

Computational models examine the physics during the collapse of a gas cloud and search for initial conditions that lead to fragmentation of the gas cloud into two components. They assume some values for conditions in the initial gas cloud including values for mass, temperature, opacity, turbulence and other values that impact collapse. Models like these tell us how the initial conditions of the gas cloud before the collapse influence the orbits and masses of the stars that form. The models can also be

used to place constraints on what types of systems would form based on a set of initial conditions. While modeling binary systems with a low mass component, Matthew Bate found that for a set of initial conditions, based on estimates of star forming conditions, that the low mass companion would not form closer than 10 Astronomical Units, the distance from the Earth to the Sun, to the primary star (Bates 2000). Accurate measurements of brown dwarf systems, including their mass fraction and orbital radius, help place constraints on formation models that help us better understand the formation of low mass objects.

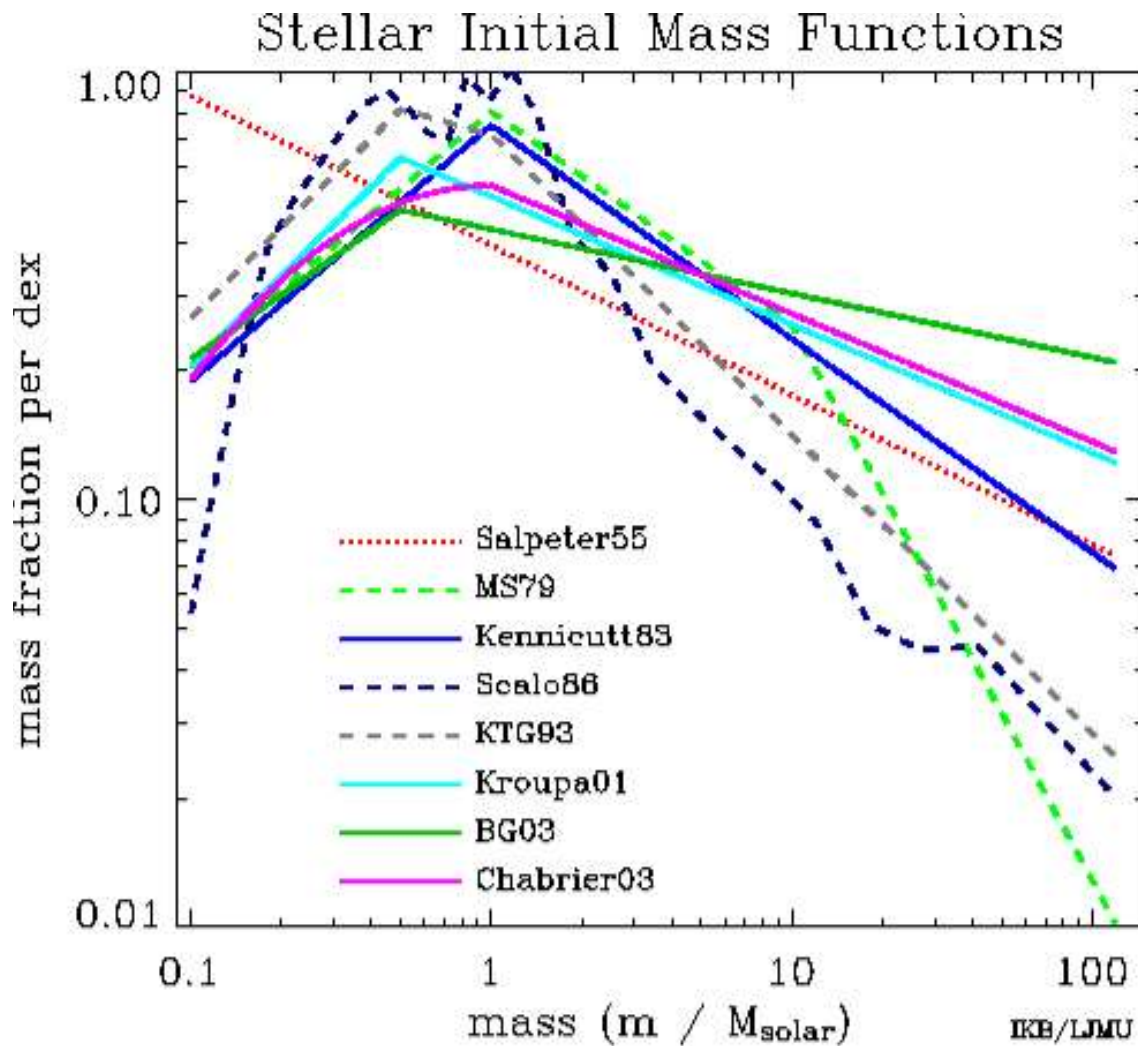


Figure 1: Initial Mass Function

Several models for the initial mass function of stars. Each line on the figure shows the function determined by a different paper given by the name and year on the figure. The x axis shows the mass of the object as a fraction of the solar mass and the y axis shows the fraction of stars at that mass. Most models peak in the same region but fall off at different rates (Chabrier 2003). Note the large differences between the models at the high and low mass end of the models.

1.1.2. Spectral Types

As brown dwarfs cool the equilibrium points for chemical reactions in their atmospheres shift. This equilibrium shift means that different molecules exist in brown dwarfs of different temperatures. An

example of this is the equilibrium shift that decreases the amount of CO and increases the fraction of methane as the object cools through the reaction in equation 1.



This occurs because as the Brown Dwarf cools the equilibrium of this reaction shifts to the right and produces more CH₄. Another important abundance is the fraction of N in N₂ compared to the amount in ammonia.



These shifting abundances create different spectral features as a function of temperature as the equilibrium shifts. The observation of these spectral differences lead to the establishment of the L, T and Y spectral types for brown dwarfs (Kirkpatrick et al. 1999) (Cushing et al. 2011). At higher temperatures features produced by CO dominate the spectra. At lower temperatures the spectra is dominated by methane and ammonia. Each of these spectral types was established by comparing the flux ratios of different spectral features. Each of these spectral types is divided into 10 subsections ranging from zero to nine where zero represents the hottest object in that spectral type.

By determining which spectral class a Brown Dwarf falls in you can get an estimate of the surface temperature of the object. There are still uncertainties in this estimate because of mixing and cloud features in the atmosphere but identifying two objects as belonging in the same spectral type allows the assumption that they have a similar temperature. Objects of the same spectral type all have similar temperatures and because these are electron degenerate objects they have similar radii, but not the same mass (Sorahana Yamura & Murakami 2013). The luminosity of a brown dwarf is a function of its surface temperature. This means the luminosity of two objects in the same spectral classification should be very close to the same value with any differences coming from slight differences in age, initial mass, and cloud structure of the object. Knowing these systems should all have

similar luminosity's allows us to look for systems that are brighter than other ones in their spectral class. We will discuss several reasons that could give us this overluminosity in the second chapter of the paper.

1.1.3. Brown Dwarf Archives

Brown Dwarf publications tend to focus on individual objects which results in many publications to look through before you find the information on the objects you are interested in. Chris Gelino assembled all of the known brown dwarfs into a single spreadsheet to allow convenient access to the available data. This database allows for the direct examination of the majority of known brown dwarfs and contains names, coordinates, spectral types and some magnitudes for 2500 (Gelino Kirkpatrick & Burgasser 2004). The magnitudes in this survey are the apparent magnitudes observed for these objects from a variety of surveys. The apparent magnitude of an object is a measurement of how bright the object appears to an observer here at Earth. We utilized the coordinates for brown dwarfs in this archive to extensively search other databases describe in this paper for observations not included in the current archive. This data will be added to the current archive in the future.

1.2. Historical Binary Searches

In the past searches for binary Brown Dwarf systems was done by using several nights of data on a large telescope to visually determine if there were two objects. After observing two distinct sources these objects required several sequences of followup observing before they can be considered confirmed as they must be shown to be comoving, moving together across the sky with the same proper motion, or see signs of orbital motion (Burgasser et al. 2005).

1.2.1. Observing Brown Dwarfs with The Hubble Space Telescope

The Hubble Space Telescope (HST) is one of the best instruments to directly detect binary systems. Hubble has an extremely low plate scale, .05 arcseconds per pixel for the Advanced Camera for Surveys (ACS) Wide Field Camera (WFC) (Dupuy & Liu 2017), so it is able to resolve very closely spaced objects (Burgasser et al. 2005). Other instruments have different resolutions with Nicmos having .045 arcseconds per pixel and the WFC3 IR camera having .1 arcseconds per pixel. Its nature as a space telescope also gives it a distinct advantage over other telescopes as it avoids some of the resolution problems the atmosphere introduces into these observations.

1.2.2. Ground-based Searches for Binary Brown Dwarfs

Binary searches are also performed on Earth using several large telescopes such as Gemini or Keck with adaptive optics (AO) (Dupuy & Liu 2017). These observations are challenging because the atmosphere makes it more difficult to resolve separate objects. This is why large telescopes typically perform the searches using AO, which allows the mirrors to correct for and remove atmospheric effects. This allows KECK to achieve angular resolutions comparable to HST with plate scales of as low as .013 arcseconds per pixel (Dupuy & Liu 2017). However, this sort of search is restricted to the largest ground based telescopes as smaller telescopes do not have enough light gathering power to detect these objects. Examining each of the 2500 known brown dwarfs for evidence if binarity would take an inordinate amount of time and would not represent a good time investment for these large telescopes. Because these observations are challenging and time on these telescopes is limited we propose a new method to reduce the number of targets to examine. This new method to vet the candidates we examine will allow us to spend observing time wisely and focus on examining objects with the highest chances of being binary.

1.3. Telescope Systems and Archival Data

In this section we describe some of the capabilities of the telescopes that provided the observations we analyze further in the paper. We will also discuss the Infrared Science Archive and how it enabled obtaining the data.

1.3.1. Global Astrometric Interferometer for Astrophysics (GAIA)

The GAIA telescope is a space telescope launched by the European Space Agency to determine astrometric parameters for hundreds of millions of objects in the Milky Way and beyond (Gaia Collaboration et al. 2020). It is an optical telescope as it was designed to focus on stars on or near the main sequence. It measures the positions of stars to a high degree of accuracy over several years of observing. These observations allow the satellite to track how much the stars move and what portion of that movement is due to Earth's motion around the Sun. This allows for the measurement of the parallax angle, the angle the stars appear to move because of the Earth's motion, which allows us to find the distance to these objects. GAIA also measures the proper motion of objects. Proper motion is the apparent motion of a star across the sky. Because the primary component of proper motion is the orbit of stars around the Milky Way objects that have the same proper motion must be gravitationally bound in some way. Because of this GAIA has led to the discovery of many binary systems whose components are observed to be moving across the sky together. Figure 2 shows how the motion of the Earth leads to parallax.

1.3.2. United Kingdom Infra-Red Telescope (UKIRT)

UKIRT is an infrared telescope that has been used to measure parallax values similar to the GAIA survey. These observations were targeted observations taken on specific brown dwarfs and was not a

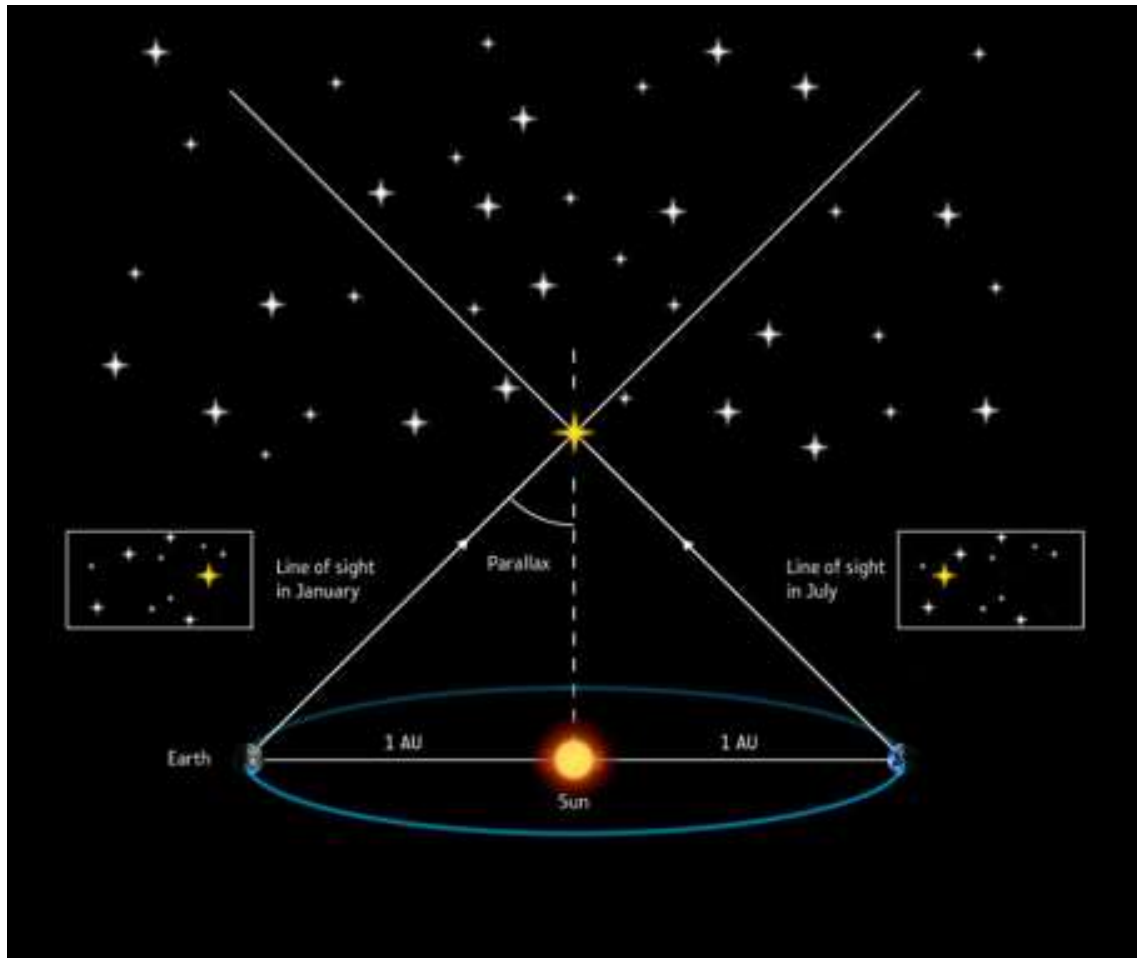


Figure 2: Parallax Using Earth's Orbit

GAIA orbits in a trajectory similar to Earth's orbit and measures parallax for many objects (ESA 2019).

general survey like GAIA (Best et al. 2020). However, since UKIRT is an infrared survey they were able to get parallax values for objects that were too faint in the optical bands that GAIA observed in. There is some degree of overlap between the two surveys and there is good agreement between the two surveys. This region of overlap and the values found by each survey are seen in figure 3. The data from UKIRT complements the data from GAIA as it focused on fainter IR sources that GAIA cannot see. This fills in the later L and T spectral types that are not observed by GAIA. This provided 60 additional objects with accurate parallax values

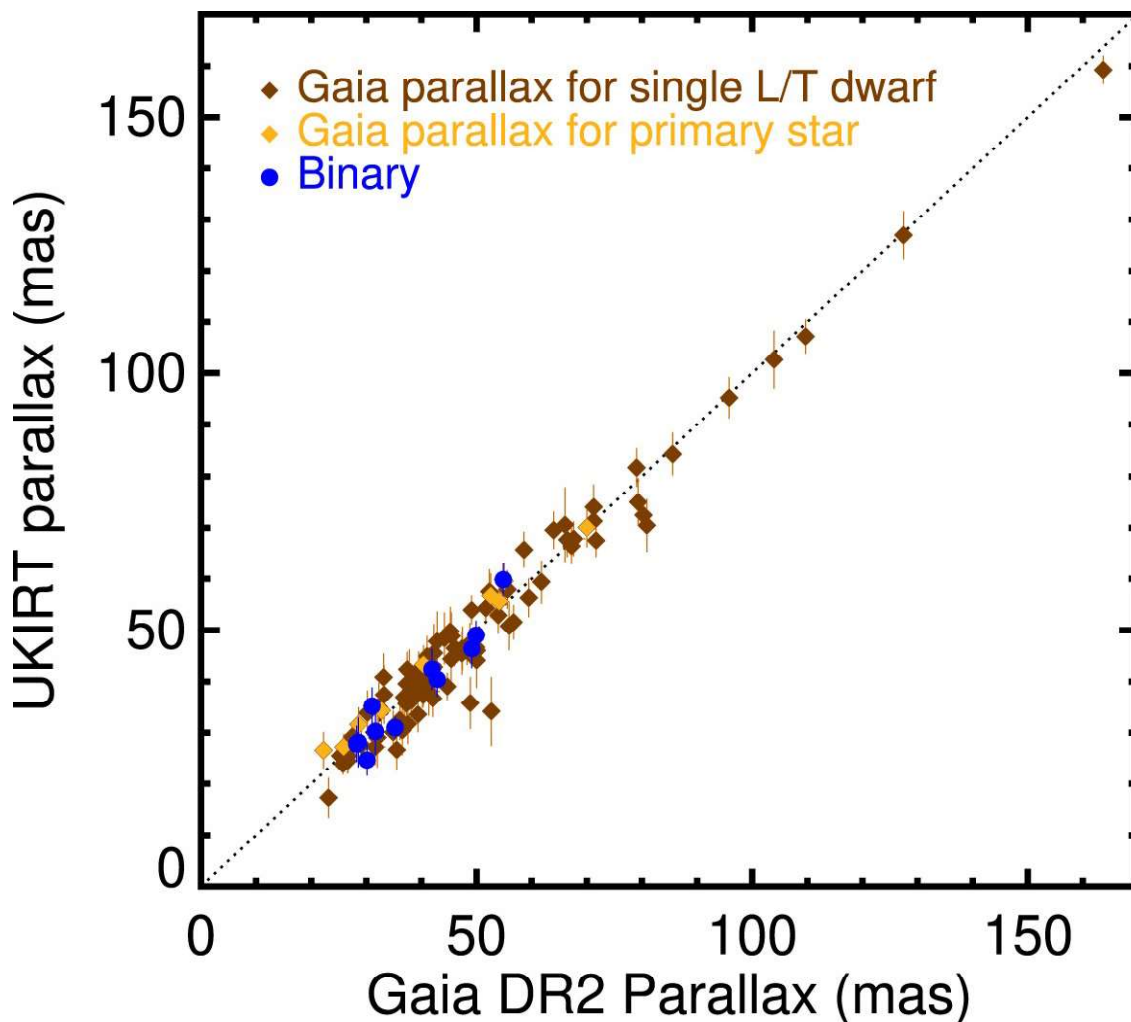


Figure 3: Comparison between GAIA and UKIRT data

The parallax measured by GAIA vs the value measured by UKIRT. The fact that the fit is linear shows there is not a systematic difference between measurements from the two surveys (Best et al. 2020). The small vertical lines through each dot indicate the error in the parallax measurement from UKIRT

1.3.3. Infrared Telescope Facility (IRTF) SpeX Spectrometer

The SpeX spectrometer, one of the main instruments on the Infrared Telescope Facility, takes infrared spectra of objects over a range of wavelengths from 1.0 to 2.5 microns. This capability to take a continuous spectra over this wavelength region made it uniquely suited to survey brown dwarfs as many spectral types have prominent features within that wavelength region. The majority of spectra taken on brown dwarfs are publicly available through the SpeX website as part of an ADAP

grant (Burgasser 2014). We use data from this as another means of examining high probability binary targets.

1.3.4. NASA Infrared Science Archive (IRSA)

IRSA is NASA's infrared science archive and maintains a database of observations from over 15 different surveys (Rebull et al. 2018). IRSA represents a large portion of what made this project feasible. Due to our large number of objects, almost 2500, searching each of the databases we have discussed in this section would be impractical. Instead we used the resources through IRSA to search for groups of our objects in several surveys. This allowed us to search for data from the GAIA, 2MASS and WISE surveys much more efficiently. This presented problems of its own which we will examine in more detail in section 2.1.2.

1.3.5. The Two Micron All Sky Survey and Wide-Field Infrared Survey Explorer (2MASS and WISE)

2MASS and WISE are the two infrared surveys we selected to provide the majority of the magnitudes we examined during this project. We selected them because they are all sky surveys with infrared magnitudes for all brown dwarfs that are bright enough to observe (Skrutskie et al. 2006; Wright et al. 2010). These two factors allowed us to get magnitudes for over 1800 objects which provides a very large sample for our analysis. We will discuss their filter systems, magnitudes and reasons behind missing data more in section 2.3.

2. METHODS AND PROCEDURES

In this section we detail how we used the databases described above to identify possible binary systems. We will begin our discussion with the GAIA telescope and a discussion on parallax values obtained with that system. Following this we introduce parallax data from UKIRT and discuss how it helps complete the data we get from GAIA. Then we discuss infrared magnitudes using 2MASS and WISE before joining it all together for a discussion on the overluminous objects we find in the dataset we assembled

2.1. Using GAIA for brown dwarfs

To find possible binary candidates we examine brown dwarfs with known distances for overluminosity. To examine this we need the distance to objects so we can find and compare their intrinsic luminosity. This luminosity is a measurement of the sum of energy emitted by an object over all wavelength. This is impractical to measure so instead we look at luminosity within a filter profile where. These filter profiles, see figure 4 for an example, only allow light through at specific wavelengths. Using these filters you measure the flux of an object which is a portion of the overall luminosity. The most common way of expressing the luminosity of an object in a specific filter is using absolute magnitude.

The absolute magnitude of an object is how bright it would appear at a distance of 10 Parsecs from Earth and is found using the relation $M = m - 5 \log(d/10)$ Where m is the apparent magnitude of the object (see section 1.1.3) M is the absolute magnitude and d is the distance to the object. Because the magnitude scale is a remnant of when observations were done by eye smaller values are brighter than large values. Using absolute magnitude is critical when comparing these objects as the apparent magnitude is effected by the distance to the brown dwarf as well as the luminosity of the

system. We use GAIA to determine the distance to Brown Dwarf systems so we can then examine them for overluminosity. We utilize the second GAIA data release (GAIA DR2) to obtain all the data analyzed in this section.

2.1.1. Using Optical Imagers for IR objects

Brown dwarfs are cool objects with temperatures below 3500 K. This low temperature means they primarily radiate energy at wavelengths redder than 1 micron. This inherent redness, coupled with strong spectra features from atoms and molecules in their atmosphere, results in many brown dwarfs to be too faint to be observed by optical systems. Two of the three filters GAIA uses to perform astrometry only extend out to 1.0 micron and the third only reaches 0.65 microns. Figure 4 shows the transmission profiles of these filters as a function of wavelength. As a result of the faintness of these objects and other challenges in identification we were only able to find 696 brown dwarfs with good parallax values.

This restriction means the majority of objects with good parallax values are early L dwarfs as these are the brightest objects. Almost 550 of the brown dwarfs we found with good parallax values are in this group (L0-L5). The majority of the remaining objects fall in the late L, 50 objects, to early T dwarf, 20 objects, range. We also found some systems that have parallax values because the brown dwarf is a companion around a brighter main sequence star. We do not include these systems in our analysis unless the systems primary object is a late M dwarf or the system is widely spaced such that the brown dwarf component can be examined separately from the host star.

Another challenge that comes from the redness of brown dwarfs is that stars that appear much fainter in 2MASS or WISE data can be far brighter in the filters that GAIA uses. This occurs when there is a star that is close along the line of sight between Earth and the system we are interested in.

These stars can be located far beyond the brown dwarf system but because of their higher apparent magnitude in filters used by GAIA they can dominate the measurement. Figure 6 is an image of the 2M 2200-03 brown dwarf taken by the 2MASS telescope in the infrared. In this figure, it is clear that the brown dwarf is much brighter in the infrared than the star that we say in Figure 5. Near-infrared surveys like 2MASS and WISE were responsible for discovering almost all of the 2500 brown dwarfs in our table. Using the coordinates of the object found by these surveys we can search GAIA for data. However, since the surveys did not report nearby stars we needed to carefully examine the results of searching GAIA for distances to ensure the correct object was identified and GAIA was not reporting the parallax of a close star.

These systems cause additional problems as the astrometric solution for the Brown Dwarf can be affected by the positioning and distance to the nearby bright object. So for systems with close neighbors the data must be inspected carefully to ensure these data artifacts are not overwhelming valid parallax values for these objects. Data from GAIA then cannot be taken at face value for these types of objects and we need to examine them cautiously to ensure the results are believable and do not produce incomprehensible results (Gaia Collaboration et al. 2020).

Another challenge we faced in finding the distances to the brown dwarfs is that these objects are very close to the Earth, typically less than 20 pc, and thus they have high proper motion. These high tangential velocities can move outside of the search radius we are using to try to find them. These movements are of particular note as many of the objects in our survey were initially discovered over ten years ago. This means the current locations of these objects differs from the locations of their discovery. This results in the misidentification of some objects as well as some objects that are missing accurate values as they cannot be found within the survey. This meant that for some searches, more than one parallax result was returned for an object because of nearby stars within the search radius. Some systems had measurements of proper motions that allowed us to be certain

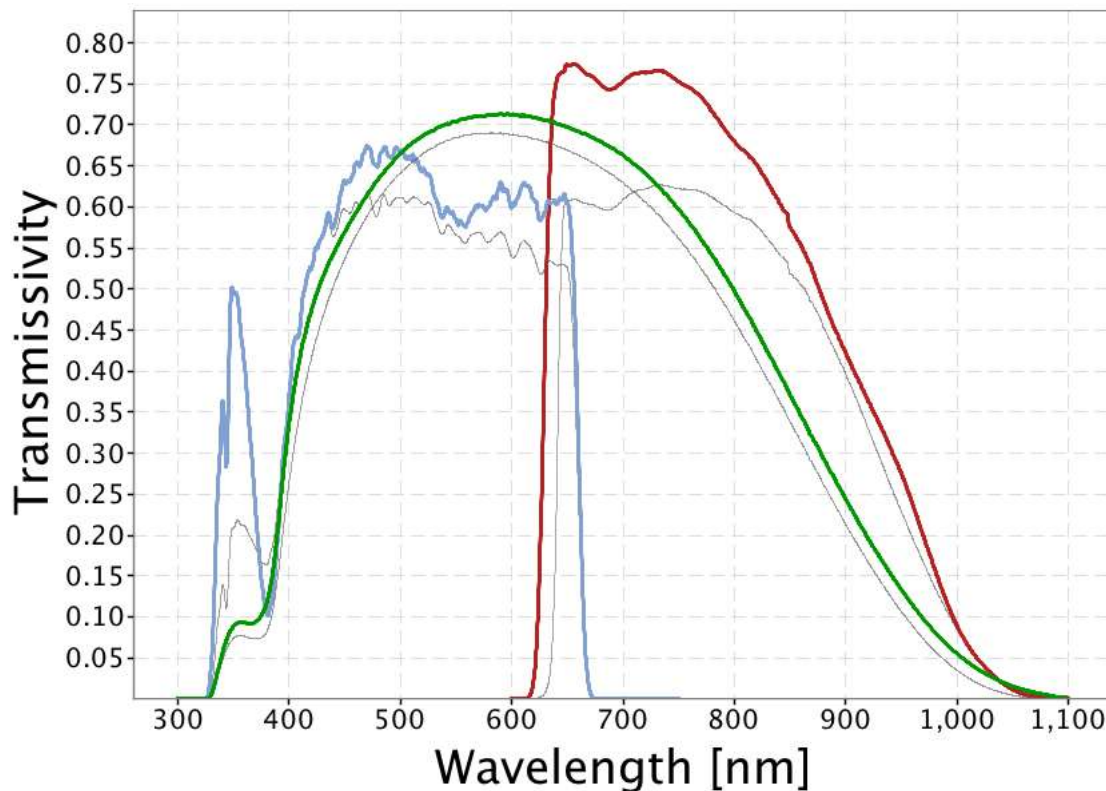


Figure 4: GAIA Passbands

Passbands for the GAIA DR2 filters. Transmissivity indicates what fraction of light at a given wavelength is allowed through the filter. The gray lines indicate the nominal filters predicted at launch and the thick colored lines describe the actual passbands of the filters (Evans et al. 2018).

we found the proper object. If there were no observations that assisted in identification we then had to visually inspect if any of the results were in fact for the brown dwarf. Sometimes the parallax did correspond to the brown dwarf, and at other times it did not.

2.1.2. Object Searching using IRSA

When examining a dataset of several thousand objects we want to spend as much time as possible analyzing and understanding the data. However, you must ensure that the data that you get is valid. When searching the GAIA database the most thorough way to ensure the data is valid is to search for each star individually using the ESA's GAIA search engine to ensure you do not run into some

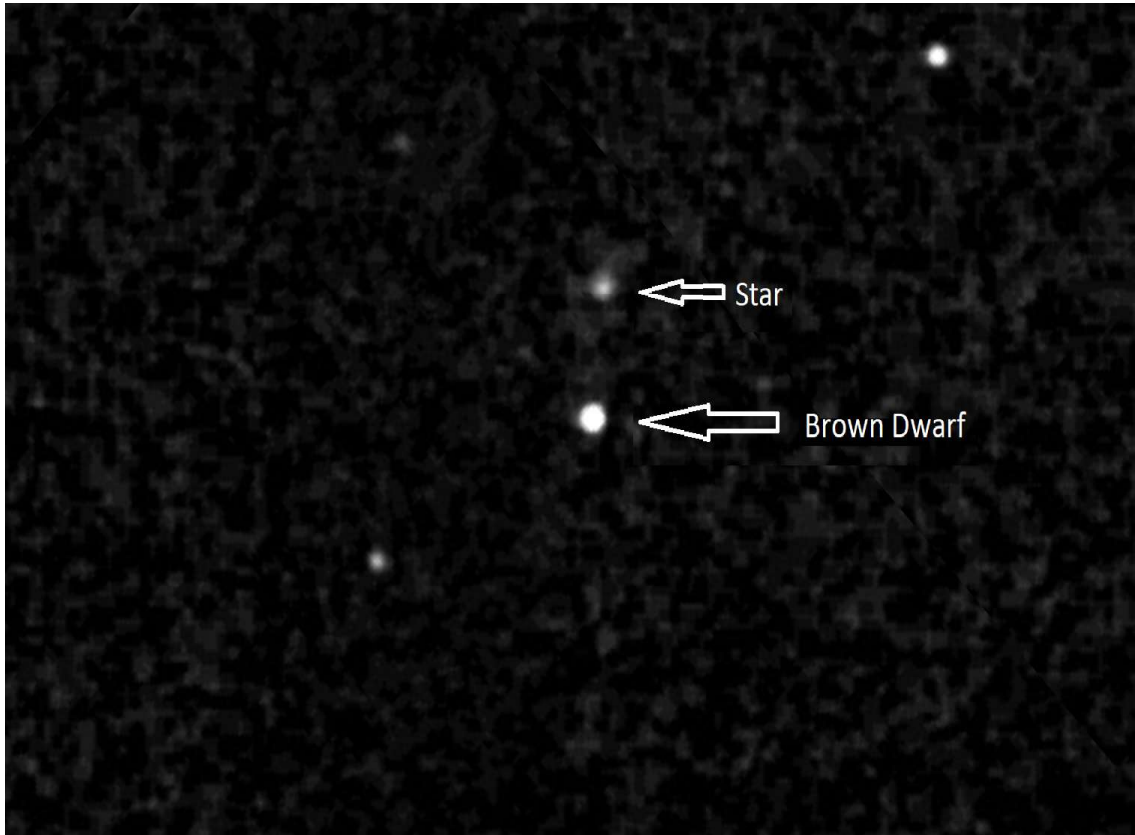


Figure 5: Infrared Brown Dwarf image

Image of a Brown Dwarf and a Star in an infrared filter (K) from the 2MASS system. This filter has a wavelength range from 19500 A (Angstroms) to 23600 A (Skrutskie et al. 2006).

of the issues we discussed in the previous section. Searches for multiple systems are possible but restrict the full functionality. Individualized searching is not an efficient methodology when you have thousands of objects to search for so we must utilize other tools in informed ways to ensure our data quality is as high as possible. Figure 7 shows the general GAIA search engine.

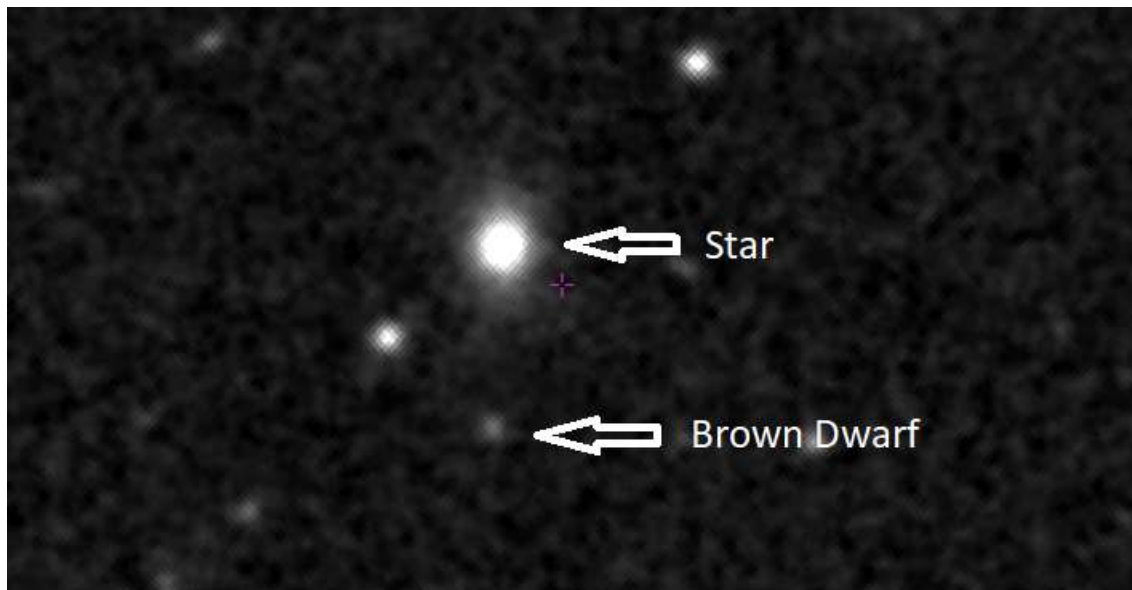


Figure 6: Optical Brown Dwarf image

Image of a Brown Dwarf and a star in an optical filter. The star, which was much fainter in the IR filter, is now much brighter than the Brown Dwarf. This image is from the Digital Sky Survey in their B filter which has a wavelength range from 3750 Å to 5500 Å (York et al. 2000).

A screenshot of the GAIA Searching interface. The interface is divided into several sections. At the top, there are two tabs: "Position" (selected) and "File". Below the tabs, there are two radio buttons: "Name" (unselected) and "Equatorial" (selected). To the right, there is a "Target in" section with two radio buttons: "Circle" (selected) and "Box" (unselected). Below this, there are input fields for "RA" and "Dec" (ICRS), and a "Radius" field set to "5" with a dropdown menu showing "arc sec". Below the search parameters, there is a "Search in:" dropdown menu with "gaiadr2.gai_source" selected. There are two expandable sections: "Extra conditions" and "Display columns". At the bottom, there is a "Max. number of results:" dropdown menu set to "500", and three buttons: "Reset Form", "Show Query", and "Submit Query".

Figure 7: GAIA Searching

Example of the individual search window used for GAIA. (ESA 2021)

To find GAIA parallaxes for all the brown dwarfs in a timely manner, we used the search engines provided by the NASA Infrared Science Archive (ISRA). This tool allowed us to search the GAIA database for several brown dwarfs simultaneously. With a batch search we needed to be careful to ensure that the data obtained was of the same accuracy as the data we would have obtained from a single object search. To maintain the integrity of our data and ensure that our targets had valid distances from GAIA we performed several searches. As a parameter for the multiobject searches in IRSA you can specify an area around each target location to search in as well as a flag to require it to only send the closest match from the catalogue. Figure 8 shows this search window and the one to one match option we utilized.

Nearby brown dwarfs have high proper motion and some have moved significantly from their discovery coordinates. To ensure the GAIA search would return values for these objects, we used several different search radii. We started with a radius of $5''$ (arcseconds) and did progressively larger searches up to $30''$. At each stage in the search if an object was found we would remove it from the list of objects to search for and then run the search again with the next search radius. This allowed us to ensure we had the sources that were closest to the locations of the target while allowing us to find sources if they had a high proper motion and had changed positions relative to their original locations. Using these search parameters we obtained parallax values from GAIA for over a thousand of the brown dwarfs in our database.

These systems did not entirely escape our problem of finding large brighter sources instead of the brown dwarfs. To get rid of these objects we looked at the color of the objects and their luminosity to identify any objects that were not brown dwarfs and then reexamined those areas using the more comprehensive searching directly in GAIA to determine if we could identify the Brown Dwarf. This allowed us to correctly identify systems such as the one shown in figure 9 where the initial search identified the bright object in a red box on the right of the image. However, after noting this system

Gaia Source Catalogue (DR2)

powered by Gator

Quick Guide
Tutorial
Catalog List
Process Monitor
Program Interface

Run Query
Reset

[Single Object Search](#)
 [Multi-Object Search](#)
 [All Sky Search](#)

SPATIAL CONSTRAINTS

Upload Table: No file chosen ✖

[One to One Match](#)

Cone Search Radius: PA Axial Ratio

(0<Radius<=300 arcsec)
NOTE: A blank radius value will trigger a search for radius ("major") from the table.
But any valid value will override the table.

OPTIONS:

<input checked="" type="radio"/> Table Output	E-mail Address (optional): <input type="text" value="No email"/>
<input type="radio"/> Source Counts Only (all-sky search only)	<input type="text"/>

Run Query
Reset

Figure 8: IRSA Searching

Example of the multibody search window for GAIA using IRSA. Note the One to One match option and the search radius option.

did not fit the expected values for a brown dwarf we examined it directly and determined the object in orange was actually the brown dwarf and were able to recover the relevant data. After we finalized data verification we were left with just under 700 sources we were confident were brown dwarfs.

2.1.3. Verifying GAIA data

After obtaining GAIA parallaxes from the ISRA database, we still needed to confirm that the validity of each measurement. Brown dwarfs are so faint that several sources of noise can throw off

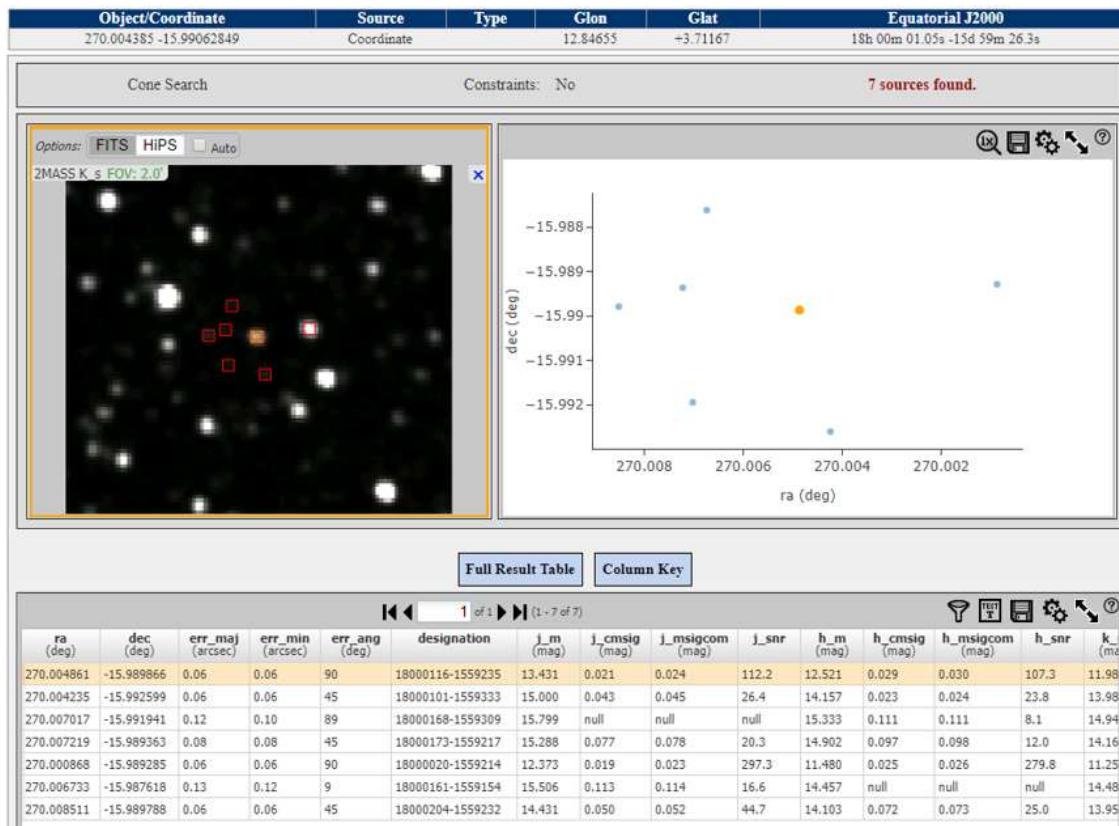


Figure 9: Search Results

Example of a system where a one to one matching search returns the incorrect object. This search identified the bright object in the red box on the right while the box in orange is the target we wanted. Searching this field using a smaller search radius or checking the field manually allows the correct object to be identified.

the validity of the final measurement. For example, uncertainties in the parallax measurement can arise from the high proper motion of the brown dwarf, the relative lack of signal from the faint brown dwarf, and errors in measuring the centroid of the brown dwarf due to stray light from nearby stars. To determine the validity of the returned results, we plotted the data and uncertainties and examined the resulting trends. Figure 10 shows the magnitude of the brown dwarfs in the GAIA g filter plotted as a function of the error in the parallax. This figure shows how there is a trend of higher parallax errors as the apparent magnitude increases. This means our estimates of overluminosity will be more effective on systems that appear brighter until GAIA has taken enough observations to drive down

the errors of these fainter systems.

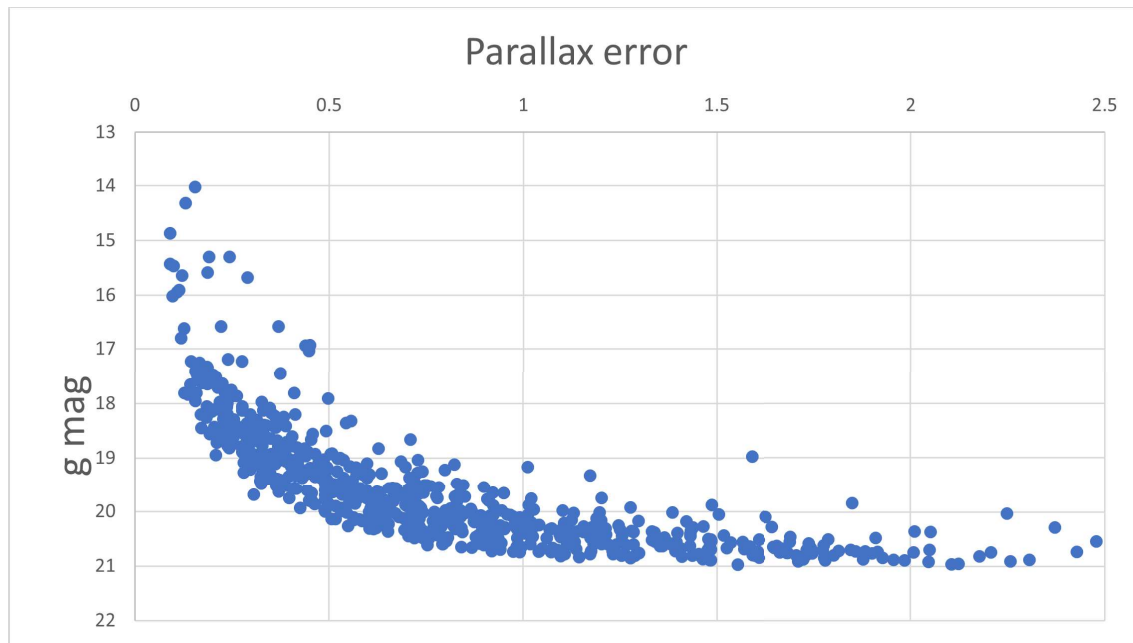


Figure 10: Data Validation 1, g apparent magnitude vs Parallax error

Apparent magnitude of the object in the g filter vs the error in the parallax in milliarcseconds

We also want to look for any sort of systematic errors to determine what their sources are. Figure 11 shows how the errors do not seem to have a dependency on spectral type. In this plot the vertical axis is a number that corresponds to the spectral type of the object. This starts from M0 which is 0 to M9 which is 9 and then continues with L and T where L0 is 10 and T0 is 20. The M8 objects seem to have a lower error overall but this is actually due to the fact that these objects are all brighter than the average object in this sample. We conclude that there is not a systematic error in the parallax as a function of spectral type and the range of uncertainties is due to the apparent magnitude discussed above.

2.1.4. Absolute Magnitudes from GAIA

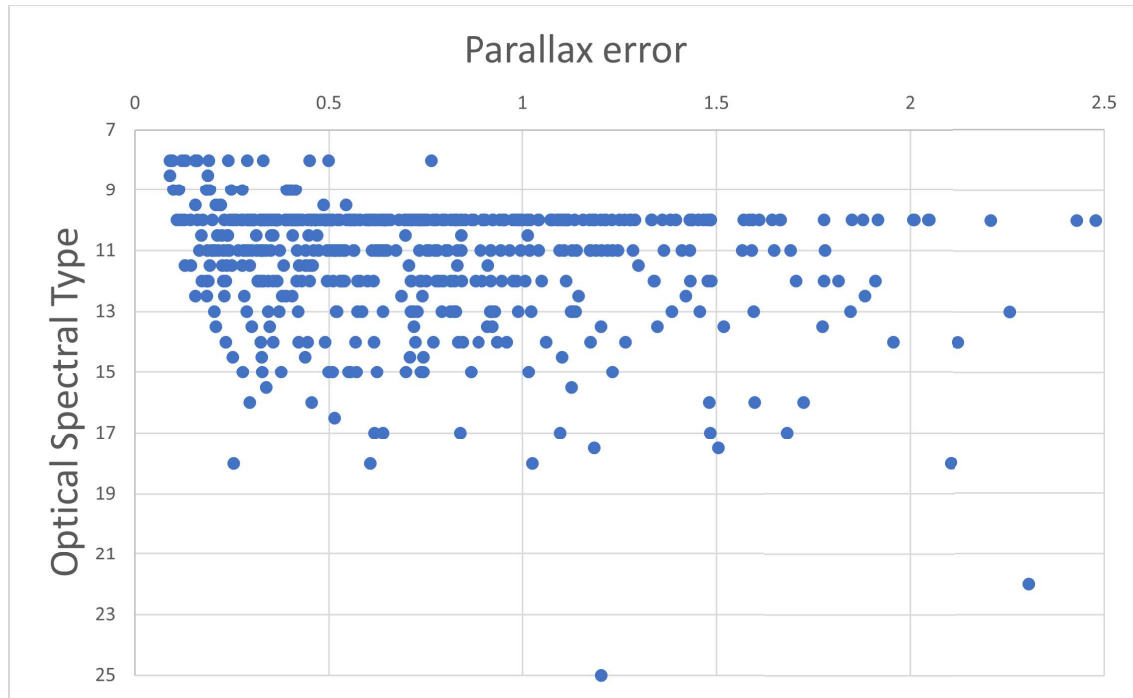


Figure 11: Data Validation 2, Optical spectral type vs Parallax error

Optical spectral type of the object (10=L0 20=T0) vs the error in the parallax measurement in milliarcseconds

To examine overluminosity we calculate the absolute magnitude of objects of the same spectral type and look for outliers. We start by examining this using the GAIA g filter. From figure 12 we can see that as you go to later and later spectral types the absolute magnitude of the object goes down. This makes sense as the later spectral types are cooler. However, individual objects within the same spectral type may just appear brighter because of differences in cloud features that make them bluer than other objects in the same type. Errors in the measurement of the parallax also will impact the calculated magnitudes. Then, to determine which of these objects are actually overluminous, we will need to use more filters to determine which objects are actually brighter.

2.2. Hawaii Infrared Parallax Program

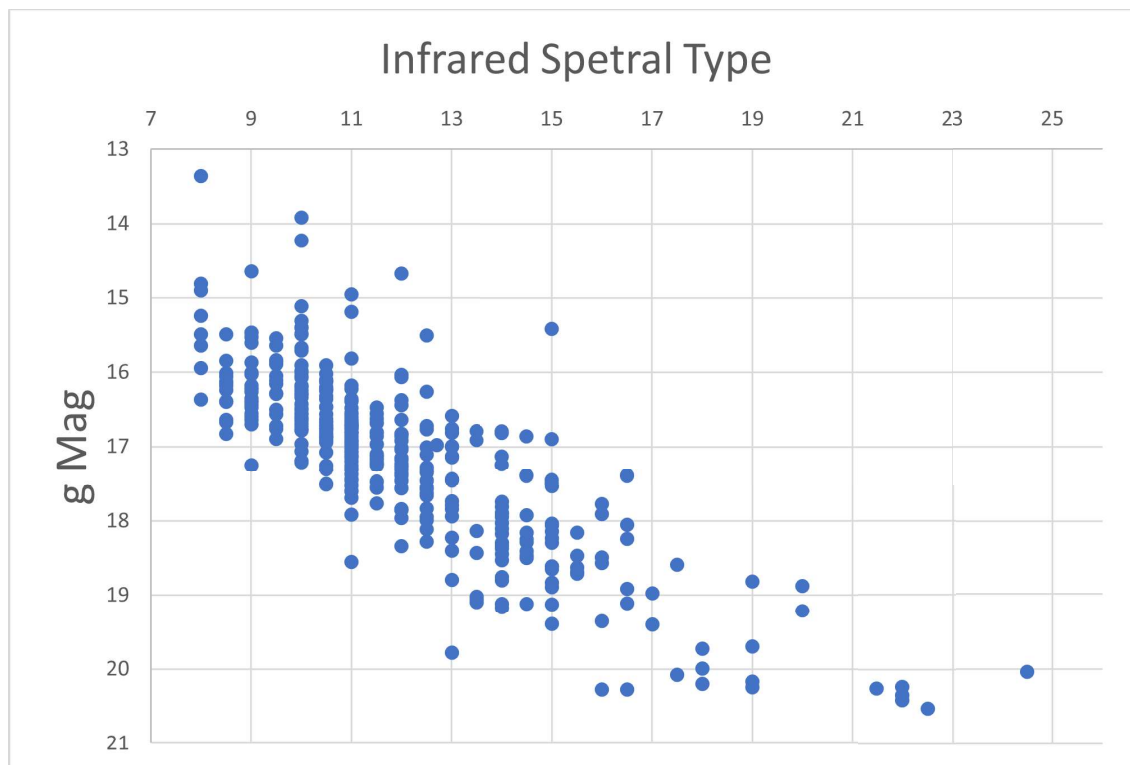


Figure 12: Data Validation 3, g Absolute magnitude vs Infrared spectral type

Absolute magnitude in the g filter versus the infrared spectral type (10=L0 20=T0)

The GAIA sample was only able to find parallax values for the brightest brown dwarfs, which tend to be the earliest L spectral types. Without any other parallax surveys, we would only have distances for this small sample of objects. Fortunately the Hawaii Infrared Parallax Program led by Will Best released a large number of new parallax measurements for the later-L and T dwarfs in the last year (Best et al. 2020). Using infrared photometry, Best was able to get accurate parallax measurements for cooler brown dwarfs. The Hawaii Parallax Program provided parallax measurements for 165 objects, and these results were included in our database to find distances for each of those objects.

The Hawaii Infrared Parallax Program used the 3.5 meter UKIRT telescope to obtain near-infrared photometry for about 384 brown dwarfs. While GAIA is able to observe the entire sky, the UKIRT telescope is located at Mauna Kea in Hawaii, and confined to observing only brown dwarfs with a declination between +60 and -40. UKIRT telescope time is also shared by several member institu-

tions, so the Hawaii Infrared Parallax Program was limited in the number of observations it could make of brown dwarfs. A total of 384 brown dwarfs were selected for observation, spanning a range of spectral types, and in general being bright enough to get excellent signal-to-noise from the ground. In the end, the final number of objects with accurate parallax values was 165 because of uncertainties in the actual measurements and for some objects an insufficient number of observations to accurately constrain the parallax motion.

Since GAIA has accurate parallax values out to the late L dwarfs there is some overlap between measurements made by GAIA and observations taken by the Hawaii program. Examining this overlap we found that, within errors, both surveys returned the same parallax value. The errors on the GAIA measurements are were smaller then the errors from UKIRT, see figure 3. This precision comes from the number of observations 100's taken to produce the GAIA distances whereas the UKIRT data was produced by using as few as 10 observations. This higher number of observations allows for a much better astrometric fit which leads to smaller errors. The errors of UKIRT were also effected by the fact that it is a ground based telescope. The atmosphere affects measurements of the centroid of the object, its central position on the sky, which increases the error relative to measurements from space. However, the UKIRT survey was able to return parallax measurements for many brown dwarfs that GAIA could not detect because they were too faint in the optical. Thus we need both the GAIA parallaxes as well as the UKIRT parallaxes to get accurate distances for as many systems as possible.

2.3. Infrared Magnitudes from 2MASS and WISE

Brown dwarfs are brightest in the near infrared so we utilized data from surveys with filters in that wavelength range to improve the signal to noise of the observations. This maximises the number of

objects we can examine while driving down errors. The 2MASA and WISE all sky surveys observed every brown dwarf at wavelengths ranging from 1 micron to 2.5 microns for 2MASS (see Figure 13) and 3 microns to 30 microns for WISE (see Figure 14). These figures show the available filters that were used for each survey. We want to utilize both of these surveys as the different filter systems cover different wavelength regions and using both of them gives us additional magnitudes to compare for overluminosity. Using multiple filters also lets us look for objects that are brighter in just one filter. We used the ISRA database to search and find 2MASS and WISE magnitudes for each of the 2500 brown dwarfs in our table. This resulted in J, H, Ks, W1, and W2 magnitudes for almost every brown dwarf. It is important to note that most brown dwarfs are too faint to reliably detect with the W3 or W4 filter so we do not include analysis of these filters as the sample size was not high.

The 2MASS survey was a ground based all-sky survey that took measurements in three filters, J, H, and Ks. These filters are standard among most ground based telescopes and were designed to operate at wavelengths where Earth's atmosphere is transparent to infrared light. Figure 15 shows the atmospheric transmission in the near-infrared and you can see that at wavelengths of 1 micron, 1.4 microns, etc. Earth's atmosphere is completely opaque to light due to absorption by the water molecules in Earth's atmosphere. Since it is impossible to receive any light from an object in space at these wavelengths, the filters were built to sit between these wavelengths. Their location maximizes the amount of signal we are able to receive from astronomical objects, while minimizing the noise produced by the atmosphere.

The WISE observations of the sky were taken by a satellite well above Earth's atmosphere. This was necessary because most of the light beyond 10 microns is completely blocked by Earth's atmosphere. Because this satellite is in space, they were able to select filters that had no real ground based counterpart. Due to their unique nature to the Wise mission, they were labeled W1, W2, W3, and W4 for Wise. The W1 and W2 filters closely resemble the ground-based L and M band filters for

easy comparison between ground and space data. But the W3 and W4 filters are unique to the Wise mission. While the W1 and W2 filters provide valuable information on the magnitude of our brown dwarfs, the W3 and W4 filters are less useful because most brown dwarfs are too faint to detect at those wavelengths.

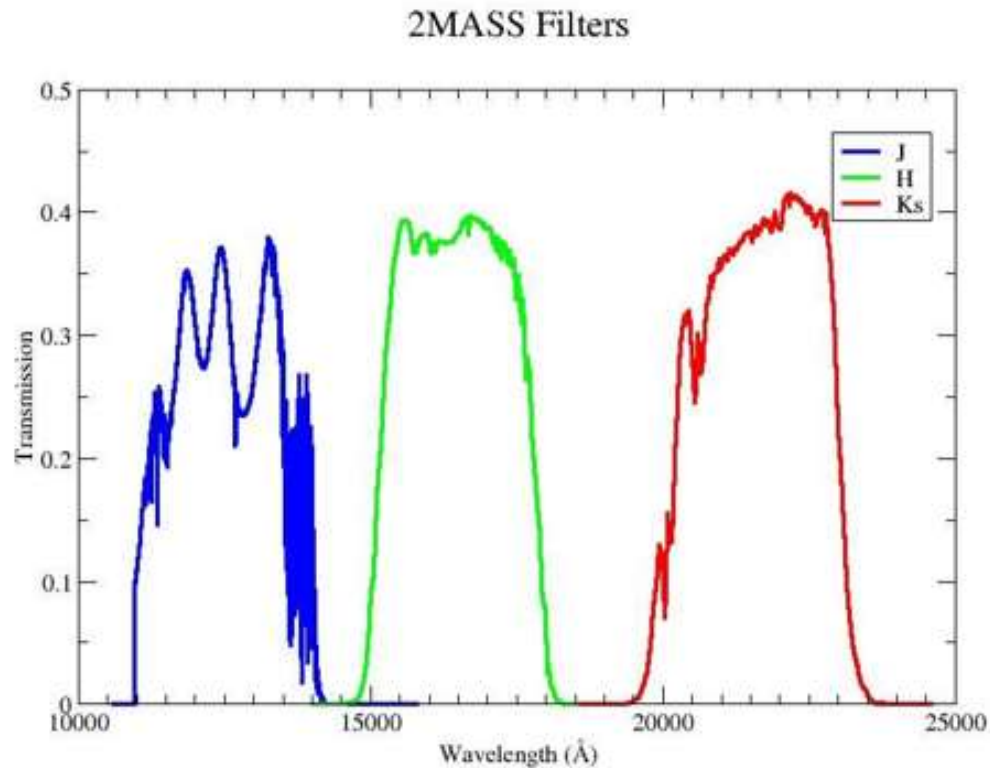


Figure 13: 2MASS Filter profiles

Filter profiles for the filters in the 2MASS system (Skrutskie et al. 2006). The blue curve is the J filter, the green curve is the H filter and the red curve is the Ks filter. The vertical axis is the fraction of light at that wavelength that is transmitted through the filter. The units of wavelength are in Angstroms.

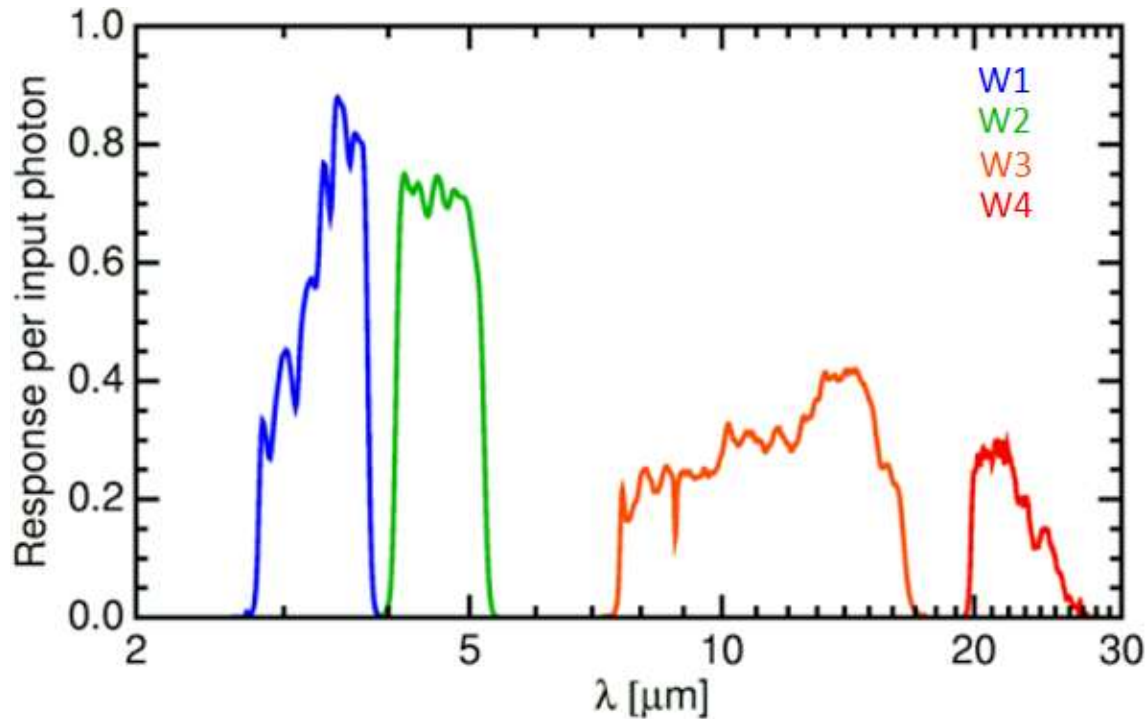


Figure 14: WISE Filter profiles

Filter profiles for the filters in the WISE system (Wright et al. 2010). The blue curve is the W1 filter, the green curve is the W2 filter, the orange curve is the W3 filter and the red curve is the W4 filter. The vertical axis gives the fraction of photons that will reach the detector which is equivalent to the transmission given above. The wavelength unit for the x axis is microns.

We used the ISRA database to search the 2MASS and WISE surveys to obtain 2MASS J, H, Ks and Wise W1 and W2 apparent magnitudes for each of our brown dwarfs. This search presented similar challenges to what we encountered when using the search engine to find GAIA parallaxes. The first issues, the object being too faint, is less present in the filters used by 2MASS and Wise because brown dwarfs are 6 to 10 orders of magnitude brighter in the near-infrared than the visible. The second difficulty, resolving which object is the source, is slightly more challenging because of the lower plate scale of these surveys compared to GAIA. To ensure we had the correct source, we analyzed the J-K color of each object that was returned to verify it fell within the region expected for a brown dwarf. If it did not fall in the expected range, we searched the nearby sky for an object

with the correct colors to find the brown dwarf.

For some of the brown dwarfs, we encountered the same problem of overcrowding of the field that we saw with GAIA. In order to identify the correct source, we combined the data from GAIA and 2MASS. If there were two objects and we were not sure which was correct, we could compare the results from GAIA with the results from 2MASS to select the object whose visible and near-infrared properties matched what would be expected for a brown dwarf. Using these surveys in parallel allowed us to verify the sources faster and with less errors. We were able to shift through the dozens of objects with confusing values and efficiently determine if they were realistic. This allowed us to find magnitudes for more than 99 percent of objects we found good parallax values for.

2.3.1. Source Verification

We are searching for magnitudes from 2MASS and WISE in the same way that we searched for the GAIA data but searching in their databases using IRSA instead. This presents challenges similar to the difficulties that we had while searching for the GAIA data. The first issue, the object being too faint, is less present in the filters used by 2MASS and WISE as they look at spectral regions where brown dwarfs are the brighter than in optical filters. The second difficulty, resolving which object is the source, is slightly more challenging because of the lower plate scale of these surveys compared to GAIA. To ensure the sources are correct we use the J-K color of the objects to ensure they fall within the region we expect for brown dwarfs. This allows us to examine the objects that have colors that we do not expect and use the data from these surveys as well as data from GAIA and the original surveys that discovered the objects to ensure we identified the correct objects.

Since these objects suffer from the same overcrowding as GAIA we can often identify the system in one of the two surveys and then use the knowledge we gain from finding it in one survey to ensure that

we find the right object in the other. Using these surveys in parallel allows us to verify the sources faster and with less errors. This allows us to sift through the dozens of objects with confusing values and efficiently determine if they are realistic or not.

3. IDENTIFYING OVERLUMINOUS CANDIDATE BINARIES

With absolute magnitudes in the 2MASS and Wise figures determined from the distance for all of the brown dwarfs with accurate parallax measurements, we were able to identify brown dwarfs that appear to be overluminous. An overluminous brown dwarf is an object that is much brighter than the other objects with the same spectral classification. There are several reasons for why a brown dwarf may be overluminous. In some cases the object simply gives off more energy at certain wavelengths. In other cases, the object has been classified in the optical part of the spectrum where the indices are sensitive to temperature. But its near-infrared spectral features are very different due to molecular and cloud opacity and if it was classified in the near-infrared it would not have the same spectral type. These opacity sources can force flux out at other wavelengths where the atmosphere is clear, making it appear brighter. A final reason could be that we are really receiving light from two brown dwarfs instead of one object, and so we are receiving twice the luminosity. An overluminous brown dwarf could actually be a binary system, and we can use overluminosity to pick the best binary candidates. We then need another technique to determine if the overluminosity is due to binarity or some other reason.

To identify overluminous brown dwarfs, we first grouped all the brown dwarfs together by spectral type, and then sorted each group from most luminous to least luminous in a given filter. Figure 15 shows such a grouping of objects for brown dwarfs with absolute 2MASS J band magnitudes. Note the general trend where most brown dwarfs have a similar magnitude within their group, but there

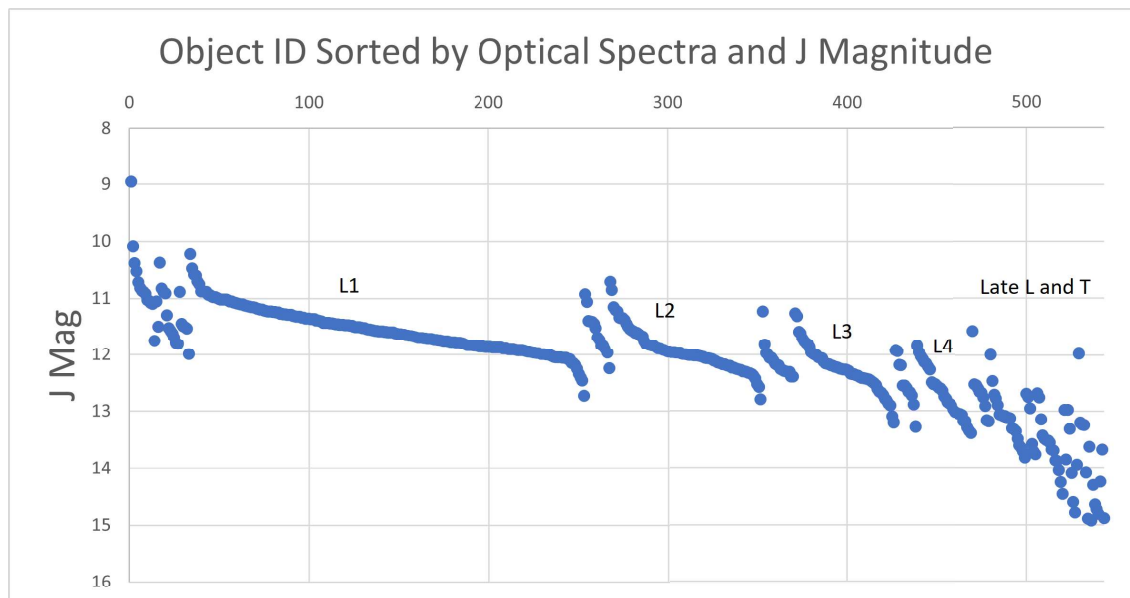


Figure 15: Results 1, J magnitude variation within optical spectral types

Individual brown dwarfs have been grouped together by their optical spectral type. Within each type we have sorted the objects from brightest J band magnitude to faintest J band magnitude. We then plotted the J band magnitude of each object as a function of spectral type, with J band magnitude decreasing to the right.

are always a handful that are much brighter or much dimmer than the rest. The differences for the first few objects in the L0 set may not look significant, but magnitudes are measured on a special logarithmic scale. A difference in magnitude of 1 corresponds to the brighter object being 2.5 times brighter in Luminosity. In the case of the L0 dwarfs, the first object is 1.3 magnitudes brighter than the average magnitude of an L0 brown dwarf, making it 3.3 times brighter than the average object. These are the objects we want to search for binarity.

While examining these objects we divided the analysis into sections and examine objects using both their optical and infrared spectral types individually. The optical and infrared spectral types differ slightly so we used both systems to ensure we were finding objects that are truly overluminous. Optical and infrared spectra differ in the wavelengths the spectra used to identify the object as well as the spectral features looked for (Kirkpatrick et al. 1999, Geballe et al. 2001). In addition, optical

spectral typing is more sensitive to temperature while infrared spectral types can be impacted by cloud opacity. So searching using both of these types can allow us to identify systems that may be binary as when there is large disagreement it is possible that we have a binary system and the flux of the colder object is influencing the spectral classification in the infrared, while the classification in the optical is still dominated by the brighter object.

Figure 16 shows how using the IR spectral type results in differences in the objects that appear overluminous. Each of the spectral types here have fewer objects as optical classification is more prevalent than infrared typing. There is a greater variance in the initial magnitude and the final magnitude in a spectral type than appears in the optical spectra plot. Differences like this show the necessity of examining both the optical and infrared spectral classifications. Using the IR spectra yielded some of the same overluminous candidates while other targets were found to only be brighter when using the IR spectra. Some of these were because they did not have optical spectra so they did not appear in our initial search.

Similar to how we examined if different spectral classifications can reveal different features we also examined using the different magnitudes from the different surveys to search for overluminous systems. To do this we plotted the data in the same way we did previously except we used a different magnitude, the one we wanted to examine, instead of the J magnitude in the y axis. So we still plotted the systems by their spectral type and then their J magnitude but plotted a different magnitude against that run of objects. This results in plots such as figure 17. From our examination of the different magnitudes we found some objects that were overluminous across all filters and others that were only brighter in specific ones.

We also want to examine overluminosity using the filters from the WISE system. As seen in figure 18 there are similar features to our graphs using the 2MASS filters. The average magnitude decreases as you go down the list in spectral types and J magnitude. However, there are many more outliers

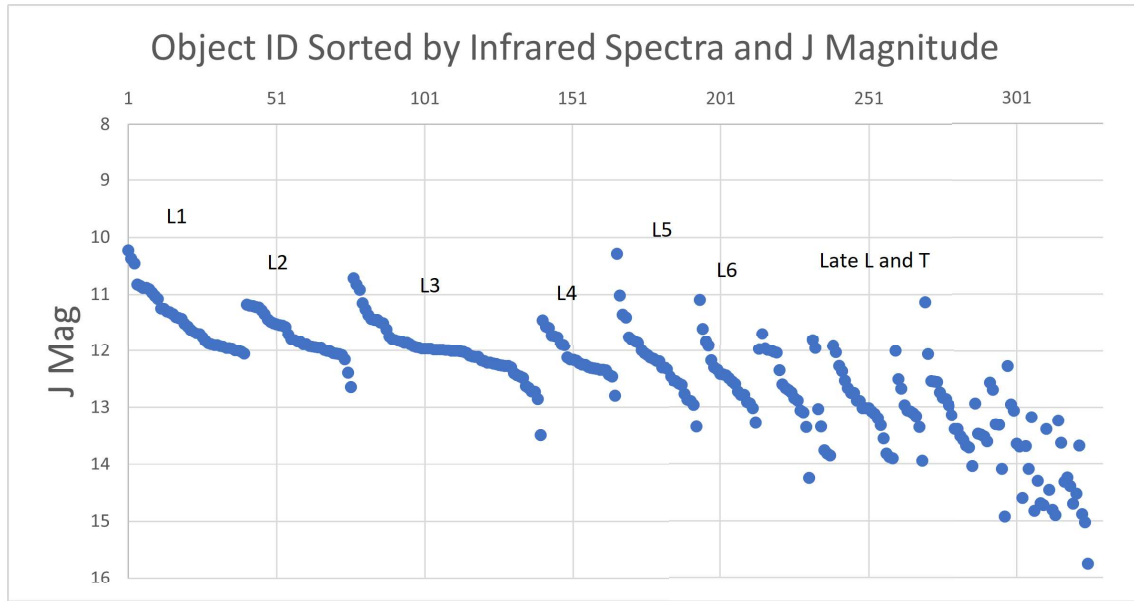


Figure 16: Results 2, J magnitude variation within infrared spectral types

Individual brown dwarfs sorted by their IR spectral type and their absolute J magnitude vs their J Magnitude.

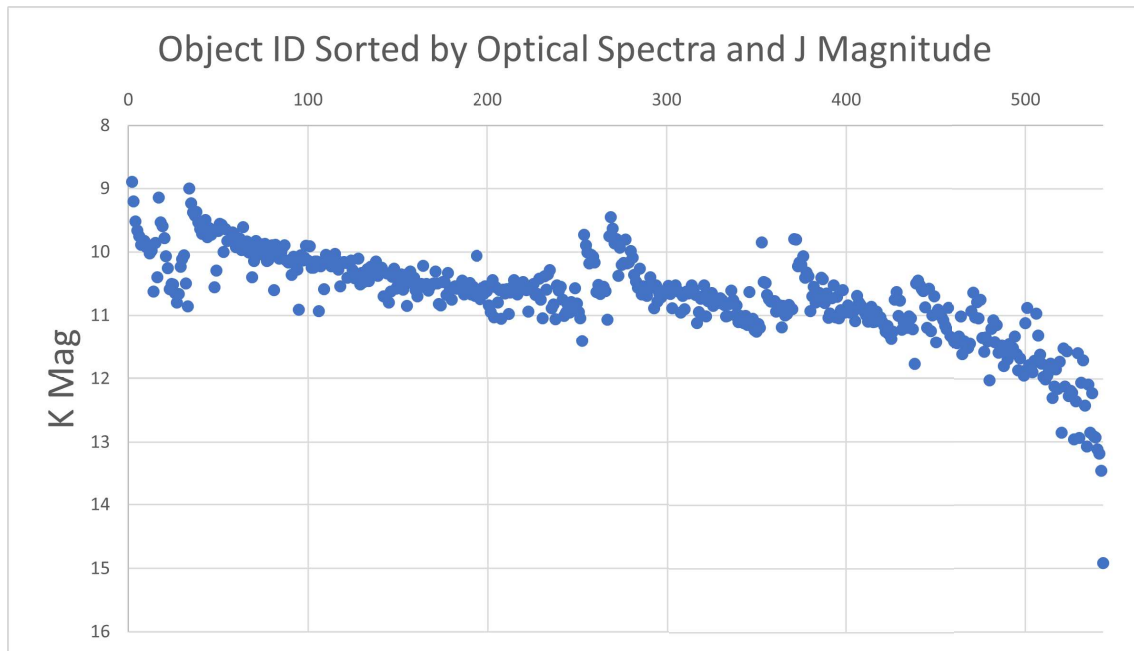


Figure 17: Results 3, Overluminosity in specific filters

Individual brown dwarfs sorted by their optical spectral type and their absolute J magnitude vs their K Magnitude

here then we saw in the 2MASS filters. This may be due to objects that are nearby that are extremely bright in the IR filters that WISE uses. This could cause misidentification of the magnitude of our objects as they are impacted by the close objects.

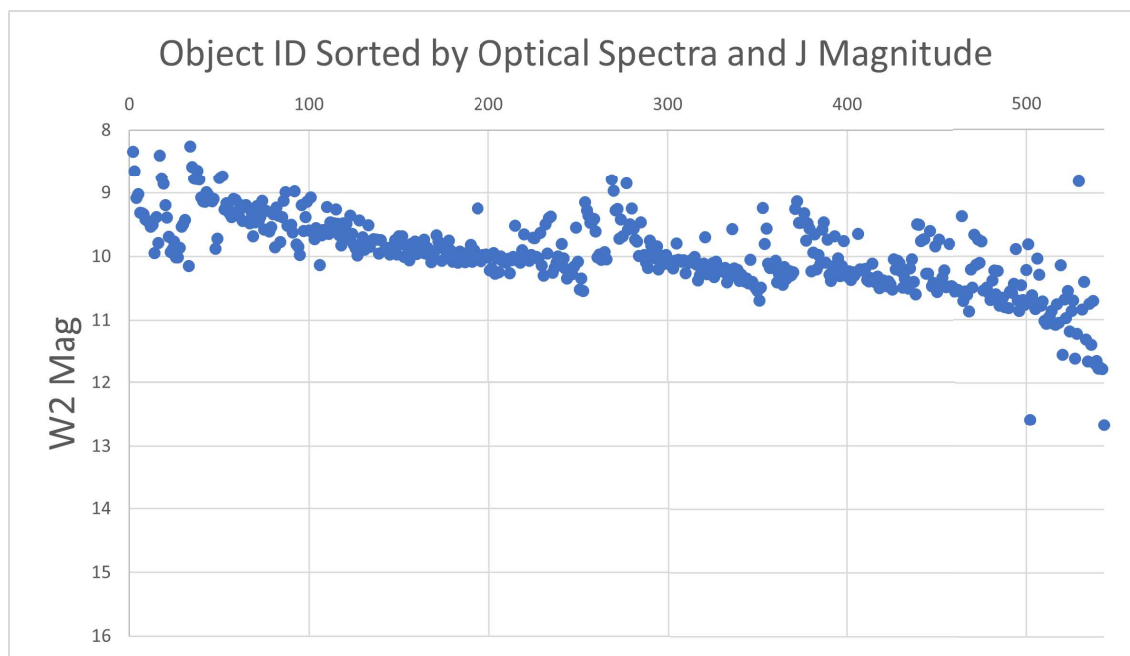


Figure 18: Results 4, Overluminosity using WISE

Individual brown dwarfs sorted by their optical spectral type and their absolute J magnitude vs their W2 Magnitude

3.1. Binaries candidates

Using each of these magnitudes we pulled the most luminous 10% of each spectral type and ended up, after we combined the data from each filter, with 90 objects that were overluminous enough that we wanted to examine the systems in more depth. With this shortened list, now less than 100 objects, we can spend time examining these systems individually with spectroscopy or high resolution photometry to determine if these systems are binary.

Not all objects that appear overluminous in our survey will necessarily be binary systems. Differences in cloud opacity, vertical mixing and differences in atmosphere structure lead to a scatter in the infrared luminosity for objects of the same spectral type. This may be a large enough difference in some cases that the objects we suspect are binary may just be extremely bright objects because of differences in their atmosphere. If the optical spectral type of an object is misidentified then it may have appear brighter than the objects of that spectral type but would actually appear average when typed correctly.

Young brown dwarfs and objects that have low metallicity will have peculiar spectra when compared to regular brown dwarfs. In the case of young brown dwarfs if care is not taken, they can be misclassified and then could appear over- or under-luminous for a given spectral type because they are young and hot and have lower density atmospheres which will affect both chemical reactions as well as chemical equilibrium and vertical mixing. Low metallicity objects will have weaker spectral features because of the lower ratio of molecules to hydrogen which leads to more emission in the infrared. These features can cause them to appear brighter than objects in the same spectral class.

Another possible reason for overluminosity is cloud variability. Brown dwarfs in the L-T region are known to have some variability associated with variations in cloud structure across their surfaces. Gaps in these clouds mean that when examining these objects we see flux from multiple layers within the atmosphere instead of just the upper layer that the optical spectral type should correspond to. This can also occur depending on what region of the brown dwarf is oriented towards us. As seen in this picture of Jupiter in figure 19, looking at the polar or equatorial regions in the infrared may cause you to over or underestimate the true luminosity of the object. This can cause the spectral type of these objects to be misidentified as the lower features can wash out the features of the actual atmosphere. If the spectral type is incorrect the object will not be compared with objects that have the same intrinsic luminosity so may appear extremely overluminous.

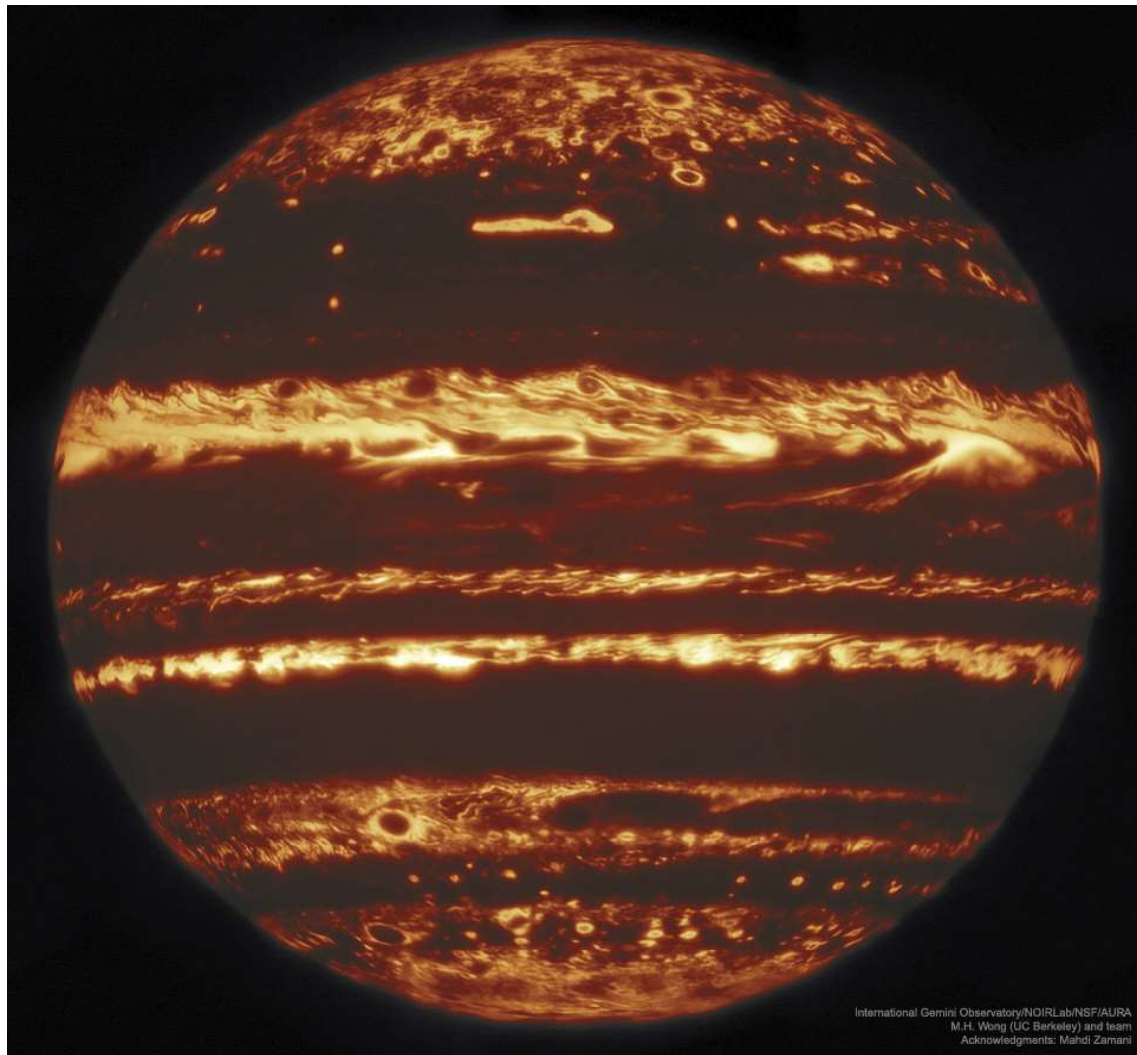


Figure 19: Jupiter in Infrared from Gemini

Image of Jupiter showing the difference in infrared flux between the equatorial and polar regions (Wong et al. 2020).

While these types of objects are not the primary reason for our search identifying these objects is also useful. Young brown dwarfs give us more insight to how brown dwarfs cool over time and variable objects help us understand the cloud structure and the equations of state that govern these objects better. It will also help us understand the occurrence of low metallicity brown dwarfs so we can probe their formation. While these are not the focus of our research identifying them allows us to establish some of these objects so future students can work specifically on these objects to improve

our understanding of brown dwarfs.

3.2. Identifying Known Binaries

There are a number of brown dwarf binary systems where both the primary and secondary candidate have been directly imaged by a telescope (Dupuy & Liu 2017, Bardalez Gagliuffi, Gelino & Burgasser 2015). If our identification of possible binary systems using overluminosity is working as we hope, then each of these known binaries should have been flagged as overluminous. These systems were resolved as two objects by telescopes with adaptive optics, but in the 2MASS and WISE images they would appear as a single overluminous object. We identified all of the known binaries that have been visually resolved in the literature and went to our list of 100 candidates to see if they were indeed overluminous for their spectral type.

Resolved binary systems with close separations are seen as a single object within surveys like 2MASS and WISE. This occurs because of the lower plate scale of these surveys which results in objects that are close to each other appearing in the same pixels. This means when we take the absolute magnitude, see section 2.1, of these objects it reflects the sum of the luminosity of the two objects. These objects should then appear brighter than the average Brown Dwarf of the same spectral type as two objects are contributing to their luminosity.

We examined several of these objects which had good parallax values within our dataset. We found that these objects were brighter than the average object in their spectral type. But surprisingly they were never the brightest object in their spectral type. The objects that are brighter could be binary systems, but they could also be young low-gravity objects, cloud-clearing objects, or objects that have very different optical and infrared spectral types due to probing different layers in the atmosphere with the spectral classification. We need to look at these objects in more detail to determine if they are binary or if some other physics is going on.

3.2.1. Unresolved Binary Systems

Brown dwarf binary systems have very small angular separations that can be just a few tens of AUs apart. This means that their angular separation can be less than 3 milliarcseconds in many cases. Even with adaptive optics, ground based telescopes are unable to clearly resolve the primary object from the secondary object and we call these binary systems “unresolved”. An unresolved binary system can only be identified as a binary if the two objects at some point move far enough away in their orbits that the telescope is able to see two distinct point-spread functions. Otherwise, all we can do is infer the possibility of a binary brown dwarf system from an examination of the spectral energy distribution.

If two L dwarfs of similar temperature are in a binary system, their combined flux will just look like an L dwarf and it is nearly impossible to tell that the object is an unresolved binary system. But their combined over-luminosity will result in our labeling the object as a likely binary system. If a binary consists of an L dwarf and a T dwarf, the extreme differences in the infrared spectra of the two objects will result in a peculiar combined spectrum that can be interpreted as possibly being due to binarity (Bardalez Gagliuffi et al.2014). These binary systems are easily identified by their peculiar spectra, but are less likely to be identified using our over-luminosity method because the increase in luminosity from adding a faint T dwarf is small. The object will just be slightly brighter than normal and may not be flagged by our methods. This means our methodology is most efficient at discovering systems where both objects are significant contributors to the luminosity of the system.

Surprisingly, one known unresolved binary system consisting of a L5 and a T5 dwarf was flagged in our search. This is not the type of system we expected to find from overluminosity and there are a few reasons for why this system is overluminous. It is possible that the L dwarf component is

brighter than expected for one of the reasons highlighted in the sections above. It is also possible that the L dwarf itself may be an unresolved binary system. If this is the case, then we have found a triple system. Further analysis would need to take place to explore why this system is overluminous.

3.3. Finding Spectral Binaries using Theoretical models

Because of the difficulties associated with this method, we determined we would need other resources to determine if these objects are binary. To do this another student examined these systems by using model Brown Dwarf spectra to simulate the spectra of these objects and determine if it was likely that they had two components (Eberhard 2020).

The atmospheric models used had a variety of astrophysical parameters that differ between the individual models. Examples of these parameters include the surface gravity and the temperature of the object. Values for surface gravity ranged from $10^{4.5}$ to $10^{5.5} \text{ cm} * \text{s}^{-2}$ (Burrows Sudarsky & Hubeny 2006). Values for the temperature of the object were drawn from 2300 K to 750 K (Burrows Sudarsky & Hubeny 2006). To determine if these objects were binary the real spectra from SpeX was compared to model spectra utilized singly and in pairs. The simulations with pairs represent the binary simulation while single objects reflect how well the spectral fit converges if there is actually just one object there.

After determining which models fit the spectra best the code examined how well the spectra could be approximated assuming there was only one object there. The code then compared this to how well the binary fits worked to return a confidence level that indicated the percent likelihood that the system is binary. Figure 20 indicates the percent confidences for 90%, 95% and 99%. The ηSB value is a distribution statistic that is a measurement of how much better the binary fits work then the single model fits and is calculated from $\eta SB = \frac{\min(\chi_{single}^2)/v_{single}}{\min(\chi_{composite}^2)/v_{binary}}$ where v is the degrees of freedom in each fit and the *chi* squared value is the value for the best fit. (Burgasser et al. 2010).

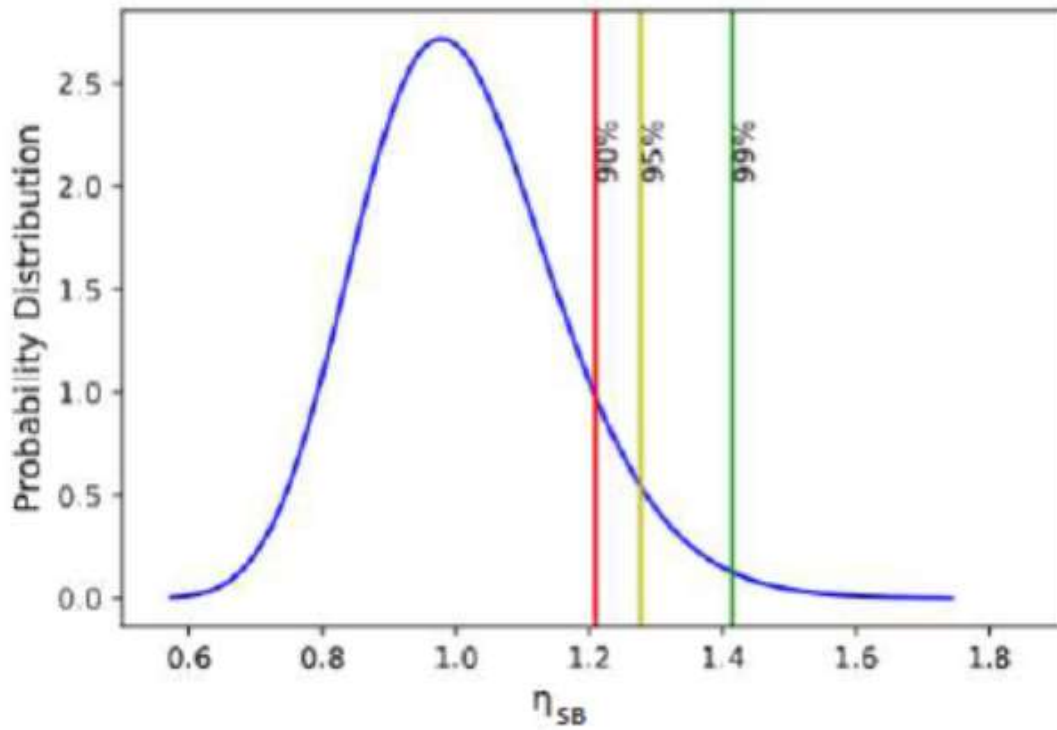


Figure 20: Spectra nSB thresholds

The η_{SB} values indicating a 90%, 95% and a 99% confidence level that these systems are binary.(Eberhard 2020)

3.3.1. Agreement with Overluminosity

To examine these systems and determine if the systems that are overluminous also have high η_{SB} 's we ran this fitting code on around 50 brown dwarfs. There were two main sections of the objects we looked at. First we examined several of the brown dwarfs that should not be binary to ensure they returned low η_{SB} 's. After doing this we examined objects that had luminosities that were significantly higher than the average luminosity for their spectral class. Most of these objects had high nSB's with binary confidence levels ranging from 90% to 99%. Because of this agreement

between the two methods we believe that luminosity is a viable way to determine if a Brown Dwarf is likely to be in a binary system.

3.4. New Brown Dwarf Archive

As part of performing this project we gathered data from several surveys for a large number of brown dwarfs. This data, while all publicly available, had not been gathered for brown dwarfs previously. After we began gathering the data for the specific objects we wanted to examine we decided to retrieve all of the data we could find so it could be used by other people examining these objects so they do not need to search for the data themselves.

3.4.1. New Data from GAIA, UKIRT, 2MASS and WISE

The main data we added to this survey were the magnitude measurements from GAIA, 2MASS and WISE. We also added parallax values for all the objects we could find in GAIA. We also added proper motions for around 1000 objects from the GAIA survey. Now instead of searching in each of these databases for this information our database allows them to find the Brown Dwarf they are looking for and then read the values they need from the table we have assembled.

3.4.2. Availability and Utility

We are currently working on publishing this database and will edit this section when it has been published. One of the biggest uses for this database is the James Webb Space Telescope (JWST). As part of the proposal process for observation time on this telescope all currently available data must be in hand to show why JWST time is needed. Our database will allow for easy access to most of

the pertinent data allowing for more time to be spent on the preparation of science proposals which will improve the quality of proposals for JWST.

3.5. Absolute Magnitude as a Binary Indicator

We have constructed a new method of identification of possible binary systems using overluminosity measurements. Because of the confirmations we have done with previously known binary objects and with spectral modeling of suspected binaries we conclude that luminosity classification does provide information on the chances of an object being overluminous. This in turn allows us to improve our estimates of the binary fraction.

3.5.1. Effectiveness of GAIA and UKIRT Parallax Measurements

The two datasets we primarily utilized to obtain distance values for brown dwarfs each have primary regions where they were more effective. GAIA was most effective at obtaining distances to L Dwarfs and very early T Dwarfs. This data was complimented by UKIRT's data which primarily was composed of late L and T Dwarfs. Late L and early T dwarfs are the spectral types closest to the transition between the two spectral types. The error bars on GAIA allowed for precise calculation of the luminosity of the objects while the slightly higher errors inherent in UKIRT made approaching the absolute magnitude of those objects a more cautious endeavor. The two datasets were both very effective in the regime that their instrumentation was designed for and by utilizing them in combination we obtained more meaningful data than either one would have provided alone.

3.5.2. Issues in Utilization of Archival Data

While we took every possible precaution to verify the data and ensure only real and accurate data was used it is possible that some of the astrometric solutions for these objects are incorrect. This data must therefore be used cautiously and verified against newer publications of distance from GAIA and other sources. In addition, because of the issues in identifying incorrect objects with this type of large scale search verifying the data you utilize become essential. We have verified all of the objects we utilized in this data as thoroughly as possible. Archival data, while supremely useful, must be treated with the appropriate level of caution to ensure you obtain real astrophysical parameters that pertain to your object.

3.5.3. Future Possibilities with GAIA DR3

The analysis done here was all performed with parallaxes from UKIRT or GAIA's Second Data Release (GAIA DR2). The European Space Agency is currently in the process of releasing the early version of the Third Data Release. The final version of GAIA DR3 will have more parallax values for faint objects as well as improved astrometric solutions for known objects. This means some of the fainter objects in our database of brown dwarfs will now have parallax values allowing for additional comparison and more binary candidates to examine. The improved accuracy will also allow searching for binary systems with faint companions as they may have much higher errors in the astrometric solution compared to single systems if the binary is widely spaced. We expect to explore this new data and determine if it allows for further insight on the binary fraction of brown dwarfs.

3.6. Conclusions

Using parallax values from GAIA and UKIRT we were successful in identifying possible binary objects within our dataset due to overluminosity. We also identified other overluminous objects and

have flagged them for photometric or spectroscopic followup to determine if they are binary. The dataset we have assembled will allow for intelligent searching of brown dwarfs for binary objects. We conclude that distance measurements from systems like GAIA and UKIRT can be used to help us understand more about brown dwarfs.

REFERENCES

- Artigau, É., Gagné, J., Faherty, J., et al. 2015, *ApJ*, 806, 254.
- Bardalez Gagliuffi, D. C., Burgasser, A. J., Gelino, C. R., et al. 2014, *ApJ*, 794, 143
- Bardalez Gagliuffi, D. C., Gelino, C. R., & Burgasser, A. J. 2015, *AJ*, 150, 163
- Bate, M. R. 2000, *MNRAS*, 314, 33
- Best, W. M. J., Liu, M. C., Magnier, E. A., et al. 2020, *AJ*, 159, 257.
- Burgasser, A. J., Reid, I. N., Leggett, S. K., et al. 2005, *ApJL*, 634, L177.
- Burgasser, A. J., Cruz, K. L., Cushing, M., et al. 2010, *ApJ*, 710, 1142.
- Burgasser, A. J. 2014, *Astronomical Society of India Conference Series*, 11, 7
- Burrows, A., Hubbard, W. B., Lunine, J. I., et al. 2001, *Reviews of Modern Physics*, 73, 719.
- Burrows, A., Sudarsky, D., & Hubeny, I. 2006, *ApJ*, 640, 1063
- Chabrier, G. 2003, *PASP*, 115, 763.
- Cruz, K. L., Reid, I. N., Kirkpatrick, J. D., et al. 2007, *AJ*, 133, 439.
- Cushing, M. C., Kirkpatrick, J. D., Gelino, C. R., et al. 2011, *ApJ*, 743, 50
- Dupuy, T. J. & Liu, M. C. 2017, *ApJS*, 231, 15
- Eberhard, JM. <https://physics.byu.edu/library/theses/2020/0> 2020
- Evans, D. W., Riello, M., De Angeli, F., et al. 2018, *A&A*, 616, A4.
- Gaia Collaboration, Smart, R. L., Sarro, L. M., et al. 2020,
- Geballe, T. R., Noll, K. S., Leggett, S. K., et al. 2001, *Ultracool Dwarfs: New Spectral Types L and T*, 83
- Gelino, C. R., Kirkpatrick, J. D., & Burgasser, A. J. 2004, *AAS Meeting Abstracts*

Kirkpatrick, J. D., Reid, I. N., Liebert, J., et al. 1999, *ApJ*, 519, 802.

Kirkpatrick, J. D., Martin, E. C., Smart, R. L., et al. 2019, *ApJS*, 240, 19

Kirkpatrick, J. D., Gelino, C. R., Faherty, J. K., et al. 2021, *ApJS*, 253, 7.

Rebull, L., Desai, V., Groom, S., et al. 2018, AAS/Division for Planetary Sciences Meeting Abstracts #50

Smart, R. L., Bucciarelli, B., Jones, H. R. A., et al. 2018, *MNRAS*, 481, 3548.

Skrutskie, M. F., Cutri, R. M., Stiening, R., et al. 2006, *AJ*, 131, 1163.

Sorahana, S., Yamamura, I., & Murakami, H. 2013, *ApJ*, 767, 77.

Wong, M. H. et al. 2020, *ApJS*, 247, 58

Wright, E. L., Eisenhardt, P. R. M., Mainzer, A. K., et al. 2010, *AJ*, 140, 1868.

York, D. G., Adelman, J., Anderson, J. E., et al. 2000, *AJ*, 120, 1579.